UNIVERSAL MECHANISM 10

MagLev Simulation

2024

Contents

1. UM Module for simulation of maglev trains

1.1. General information

Program package Universal Mechanism includes a specialized module **UM MagLev** for analysis of 3D dynamics of both single magnetic levitation vehicle and trains. The module includes additional tools integrated into the program kernel.

UM MagLev is close to the UM Monorail train module and requires it. In particular, the user may add tires to the maglev vehicle, which can be useful for modeling EDS systems.

The module is available in the UM configuration if the sign + is set in the corresponding line of the **About** window, the **Help | About…** menu command, Figure 1.1.

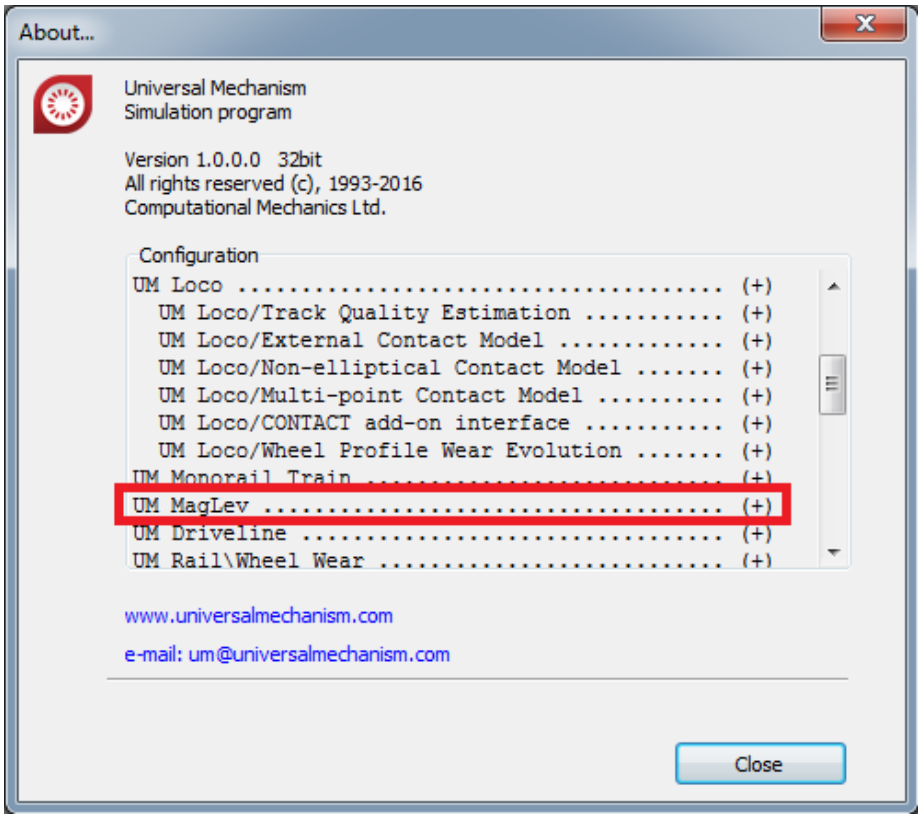

Figure 1.1. UM MagLev module is available

UM MagLev contains the following main components:

- tools for generation and visualization of guideway structure (bridge) geometry;
- tools for generation and visualization of guideway roughness (irregularities);
- mathematical models of magnetic levitation and guidance forces;
- set of typical dynamic experiments.

UM Maglev allows the user to solve the following problems:

- analysis of control system stability;
- estimation of vehicle vibrations due to irregularities;
- estimation of vehicle dynamic performances on curving;

- parametric optimization of vehicle elements according to various criteria.

1.2. Base system of coordinates

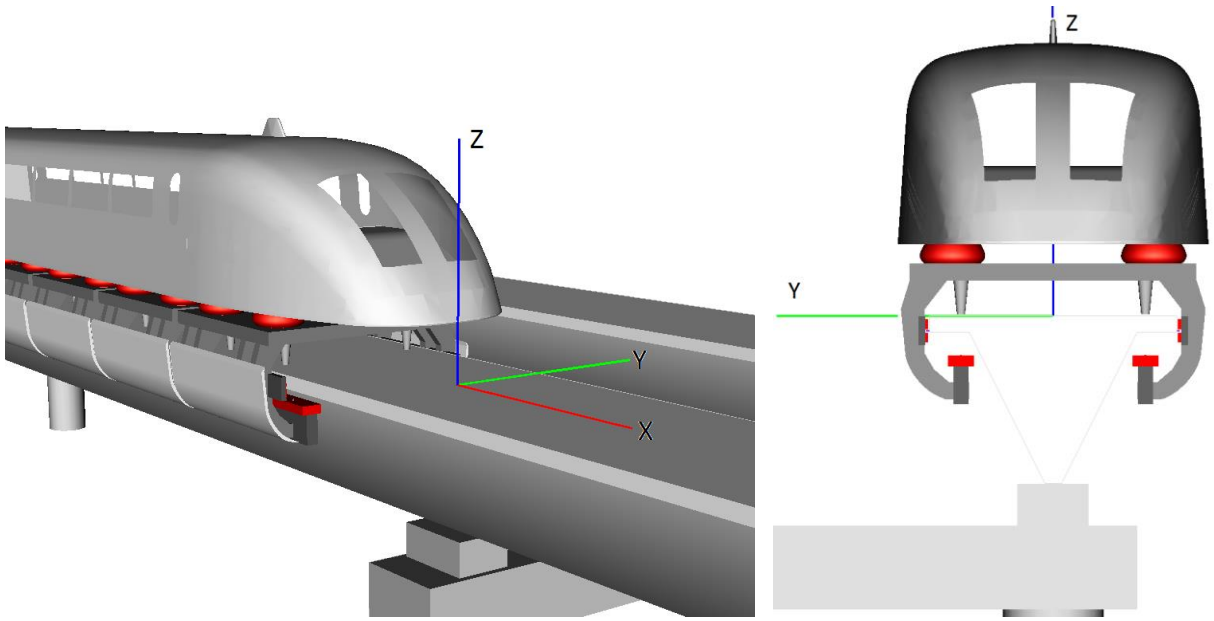

Figure 1.2. Base system of coordinates (SC0)

Inertial system of coordinates (SC0) in UM MagLev meets the following requirements (Figure 1.2).

- Axis Z is vertical, axis X coincides with the vehicle longitudinal axis at its ideal position at the moment of motion start; direction of X axis corresponds to the motion direction of the vehicle.
- Origin of SC0 lies at the centerline of the ideal upper surface of track beam.

1.3. Development of vehicle model

The user develops the vehicle model in UM Input.exe program. The model consists of bodies, joints and force element. We recommend to start the model development with studying the model delivered with UM {UM Data}\Samples\MagLev\MagLev vehicle.

1.3.1. Maglev vehicle identification

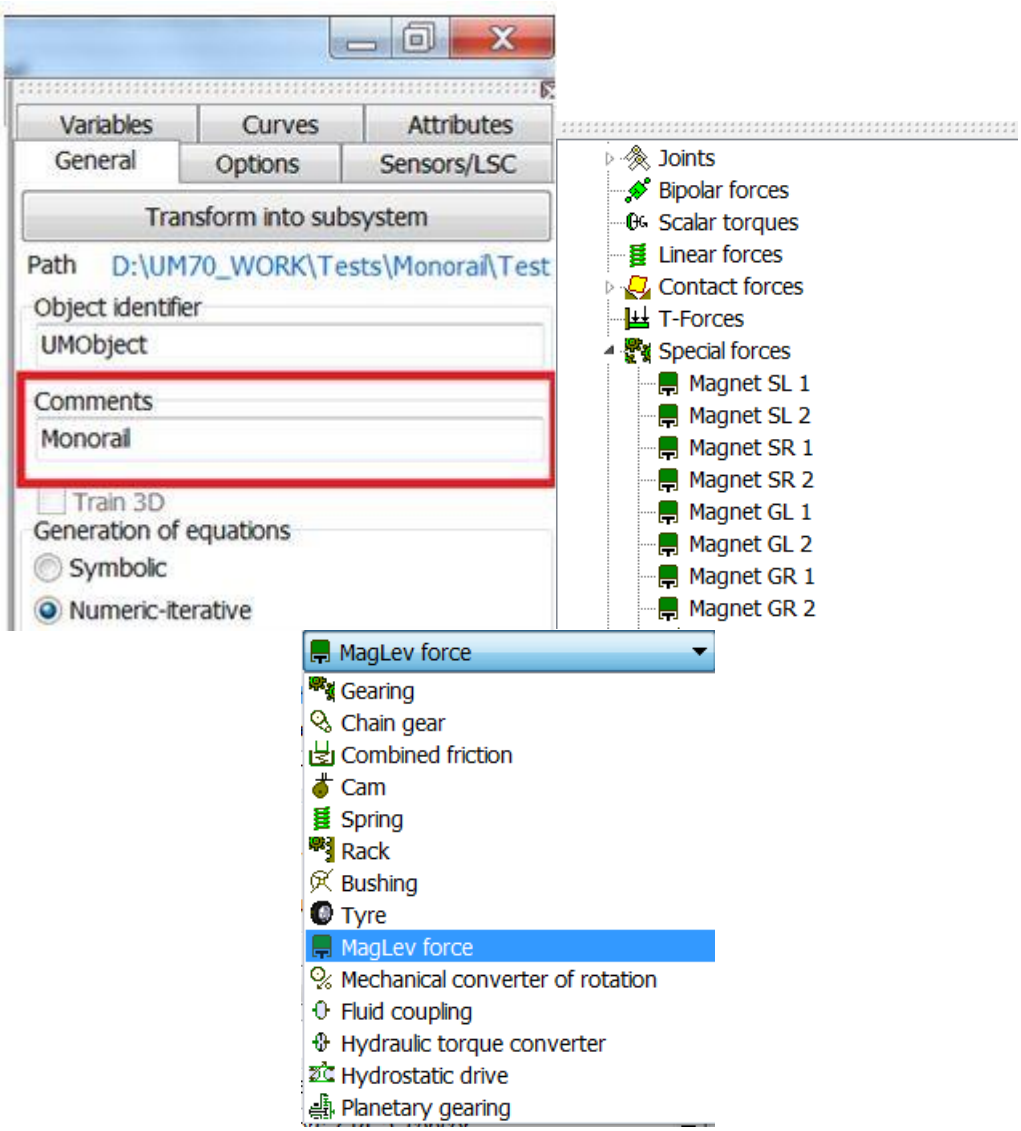

Figure 1.3. Text attribute ‘Monorail’. Special forces ‘MagLev force’

UM identifies the model as a maglev vehicle or a maglev train if the following two requirements are met in the model description:

- The standard text comment ‘Monorail’ must be set in the **Comments** box on the **General** tab of the data inspector, Figure 1.3, left;
- Special forces of the **MagLev force** type are presented in the model, Figure 1.3.

1.3.2. Modeling levitation and guidance magnets

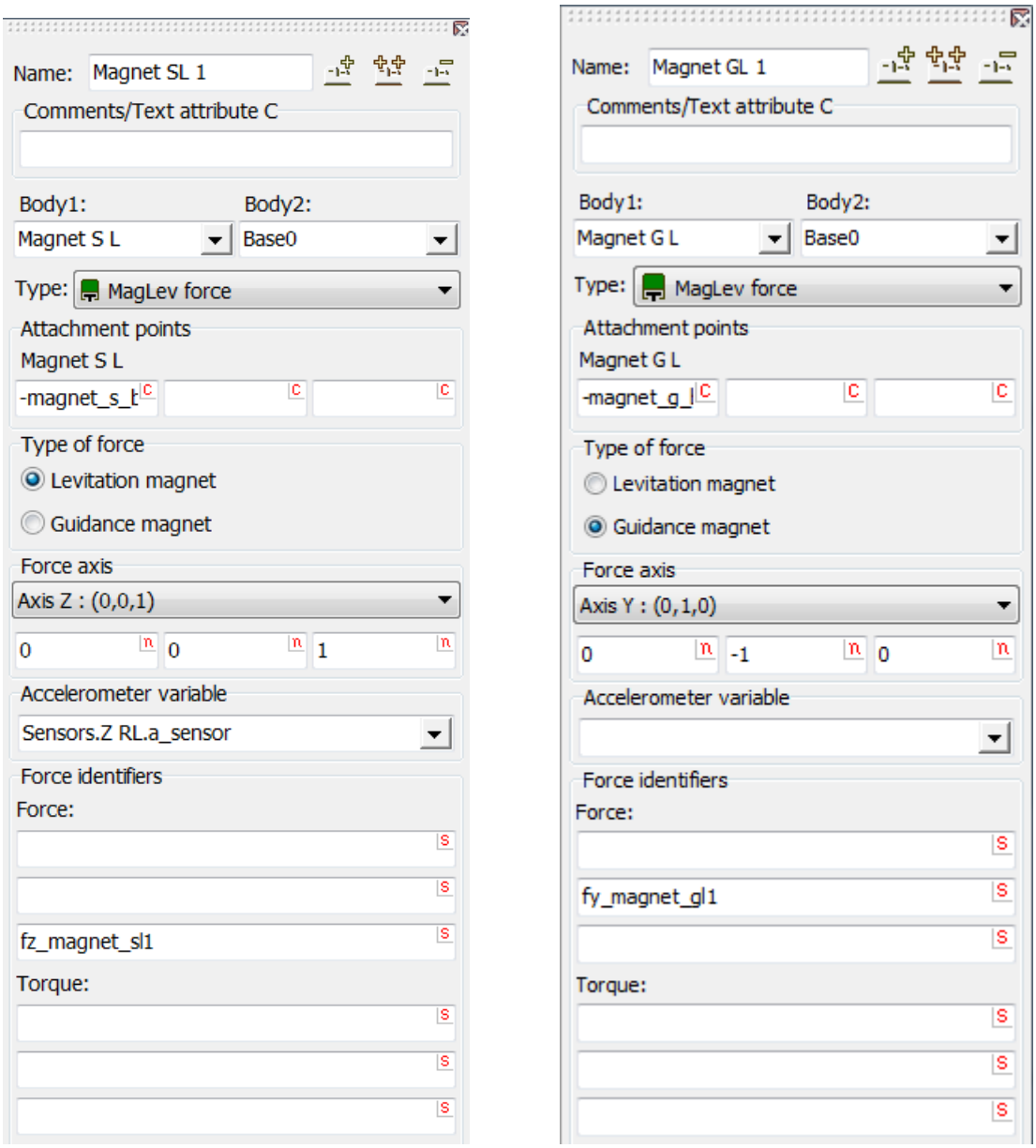

Figure 1.4. Force elements for levitation and guidance magnets

Both levitation and guidance magnets are modeled by special force elements of the **MagLev force** type, Figure 1.4.

Bodies

The first body in the force element model must be levitation or guidance magnet. The second body must be Base0.

Attachment points

The magnet force is applied to magnet at point, which coordinates are set in the local coordinate system of the magnet. The coordinates can be parameterized by identifiers.

Force axis

The force axis is a unit vector along the magnet force. As a rule, it is (0, 0, 1) the levitation magnets, and (0, -1, 0) or (0, 1, 0) for the left or right guidance magnets.

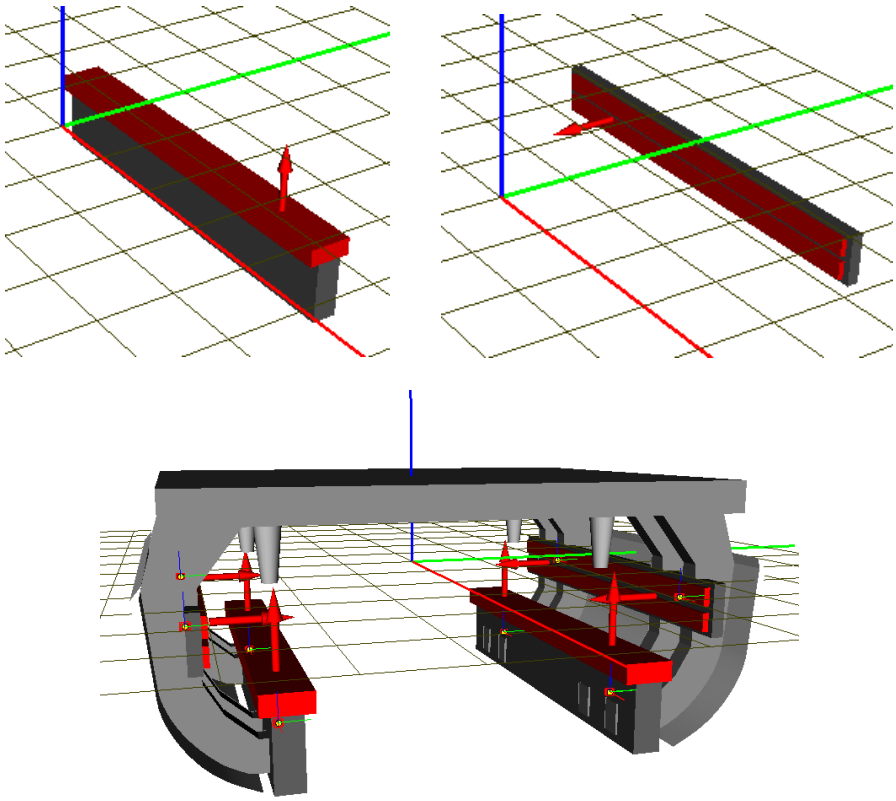

Figure 1.5. Visualization of attachment point and magnet axis

Geometric data are visualized in the animation window by a red vector, which origin and direction coincide with the attachment points and the force axis, Figure 1.5.

Type of force

Each of the force element can describe either levitation or guidance electromagnetic force. U-shaped levitation magnets can be used for a passive guidance system, Section 1.6.3 *U-shaped magnet*.

Accelerometer variable

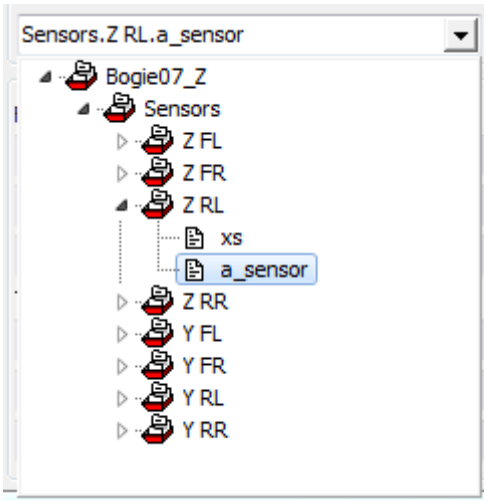

Figure 1.6. Selection of acceleration variable

Usually the magnet control includes an acceleration term, Section 1.6.2 *Single pole magnet model*. The acceleration value can be obtained from the model of accelerometer, Section 1.3.3 *Model of accelerometer*. The variable corresponding to the accelerometer data is selected from the drop down list, Figure 1.6.

Force identifiers

If force computation is implemented with Matlab/Simulink interface, *unique* identifiers must be assigned to nonzero force and torque components. The components are specified in the track coordinate system. It is not correct to assign one identifier to several force elements.

1.3.3. Model of accelerometer

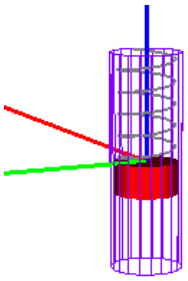

Figure 1.7. Accelerometer

Use of mechanical model of accelerometers is recommended if acceleration is included in the magnet control. An alternative computation of acceleration implements the acceleration prediction and does not allow correct linearization of equations of motion in UM.

Here we consider a standard UM model of a simplified mechanical accelerometer, which can be used in models of maglev vehicles. The model in located in the directory

{UM Data}\Samples\MagLev\Accelerometer

and describes a mass-spring mechanical system with damping, Figure 1.7.

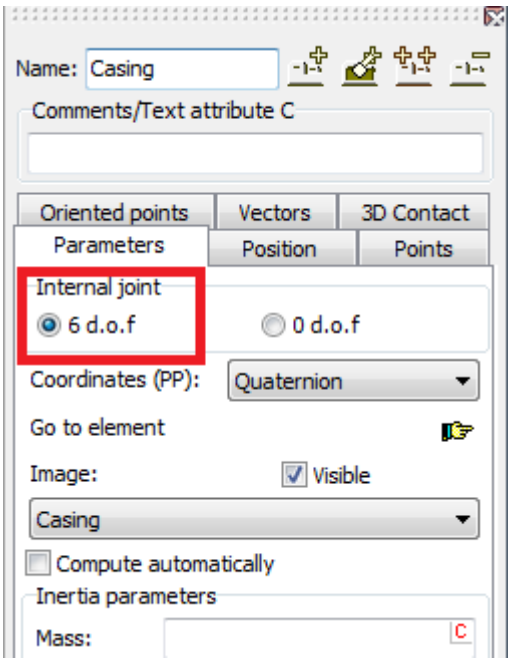

Figure 1.8. Fictitious body

The model includes a fictitious massless body **Casing** with internal 6 d.o.f. joint, Figure 1.8. This joint will be automatically removed after coupling the casing with the corresponding magnet. Other model elements are

- Body **Mass**
- Translational joint **jMass** connecting the mass body with the fictitious one; the joint allows motion of mass along the Z axis of the casing

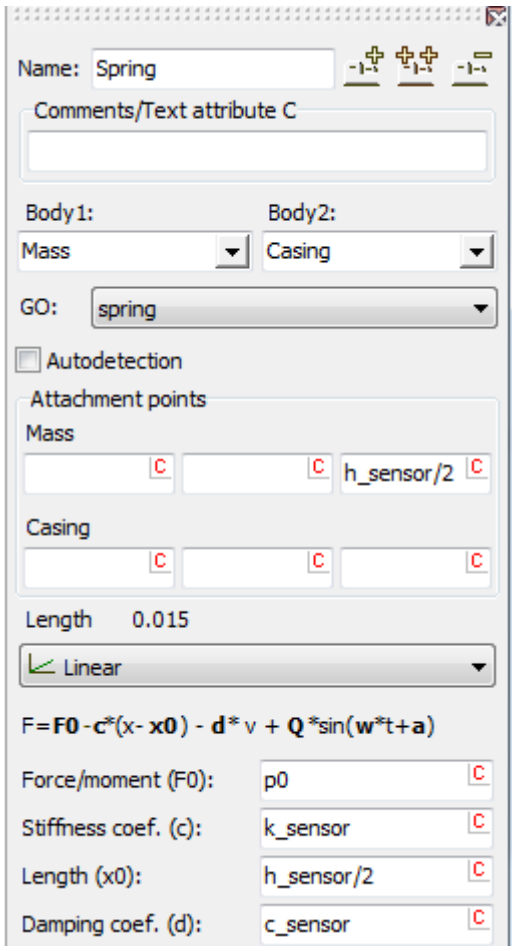

Figure 1.9. Spring as bipolar force element

- The bipolar force element **Spring** models linear spring and damping, Figure 1.9. A correct use of this element for evaluation of acceleration requires setting the stationary value of the spring force, which is parameterized by the identifier *p0*. This value is equal to the projection of the weight force of the masspoint on the accelerometer axis with the opposite sign. Thus, for vertical upward sensor orientation *p0* is equal to the weight of the mass point, and for the horizontal orientation of the accelerometer *p0*=0.

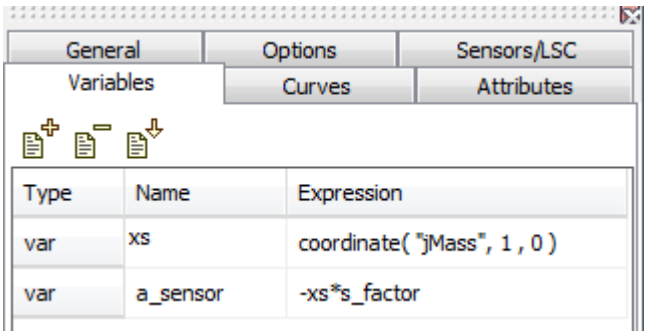

Figure 1.10. Variables

- The list of variables computes the accelerometer data. The corresponding variable is *a_sensor*.

The approximate value of measured acceleration *a* is computed according to the formula

$$a = \frac{k}{m} dx,$$

where *dx* is the spring deflection from the equilibrium position, which is presented by the variable *xs* (Figure 1.10); *k* is the spring constant, and *m* id the mass of the sensor masspoint. The ratio k/m is equal to the value of identifier *s_factor*, Figure 1.11.

Name	Expression	Value	Comment
ms	0.01		Mass
ps	ms*9.81	0.0981	Weight
beta	0.3		Damping ratio
fs	500		Natural frequency (Hz)
k_sensor	sqr(2*pi*fs)*ms	9.8696044E+4	Spring constant
c_sensor	2*beta*sqrt(k_sensor*ms)	18.849556	Damping constant
dx_static	ps/k_sensor	9.9396081E-7	Static deflection
s_factor	k_sensor/ms	9.8696044E+6	Acceleration factor
r_sensor	0.005		Casing radius
h_sensor	0.03		Casing length
p0	0		Static force

Figure 1.11. List of identifiers in accelerometer model

Parameterization of the accelerometer model by identifiers is shown in Figure 1.11.

1.3.4. Sliding contacts

Sliding contact forces are used for modeling contact interaction of vehicle with the track. The corresponding force element is the **Points-Plane** contact, Figure 1.12.

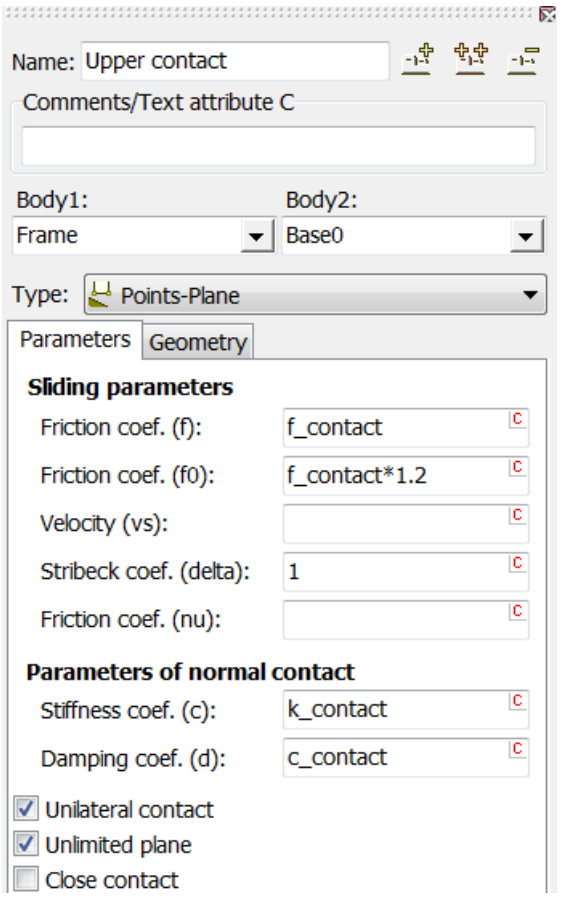

Figure 1.12. Example of sliding contact

The sliding contact at each of the contact points produces a normal and a friction force between one of the vehicle bodies (i.e. a bogie frame, a magnet holder) and the **Base0** body. Contact points are assigned to the first body, ant the plane belongs to the track. The plane normal is defined in the track system of coordinates moving together with the vehicle. The origin of this moving system of coordinates follows the projection of the contact body center of mass on the track centerline.

The sliding contact can be used for modeling

- equilibrium position of vehicle with disabled levitation magnets;
- bumpstop elements in lateral and vertical directions.

Contact forces should be described as *unilateral* ones, Figure 1.12. Necessary gaps between the contact points and the contact plane must be foreseen, see Section 1.4.1.7. *Sliding contact elements.*

1.3.5. Accelerometer positioning

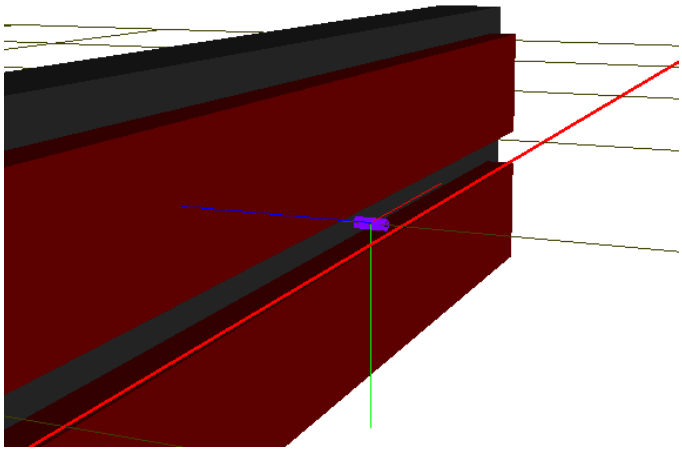

Figure 1.13. Accelerometer fixed to a guidance magnet

A necessary number of accelerometers are included to the maglev bogie model as included subsystems. The accelerometer casing is fixed to a body, which acceleration should be measured, Figure 1.13.

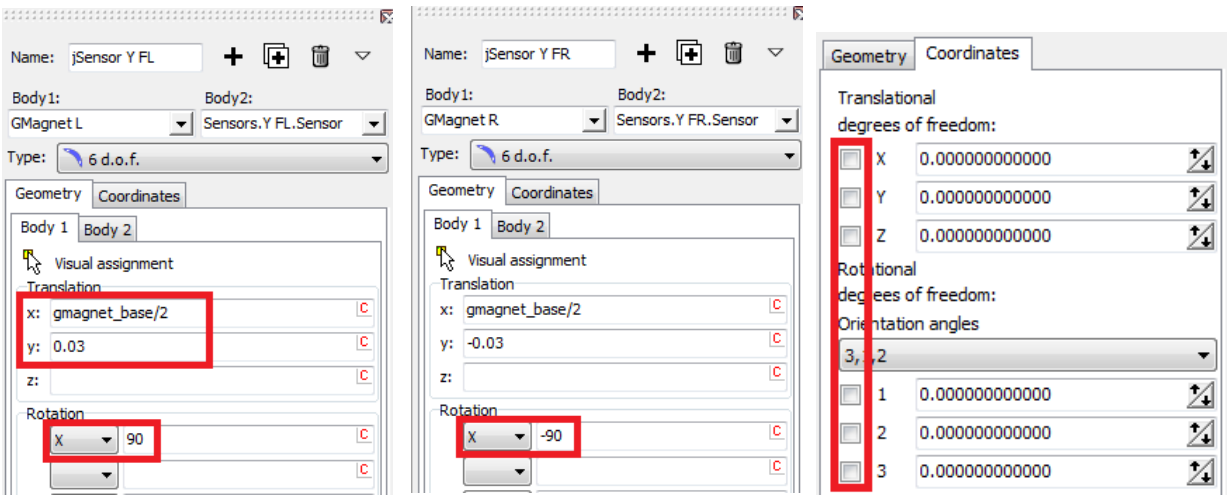

Figure 1.14. Sensor fixing to guidance magnet by a joint

A joint with zero d.o.f. is used to set the sensor in desired position and orientation, Figure 1.14. The first body in the joint is a magnet, and the fictitious body **Casing** in the sensor model is assigned as the second joint body.

The joint shift for the first body specifies the accelerometer position. In the case of a guidance magnet, the accelerometer axis must set in the horizontal direction, which is done by a rotation on 90° about the X axis for the left magnets and on -90° for the right ones, Figure 1.14.

1.3.6. Vehicle suspension and standard force elements

Suspension elements are models with standard force elements such as *generalized* linear force elements, bipolar force elements, bushings and so on. More information can be found in the file Chapter 26.

1.4. Maglev test models

Here we consider models of maglev vehicles, which allow the user to verify the correctness of simulation with UM MagLev and to get experience in development and analysis of maglev vehicles.

1.4.1. Maglev bogie model

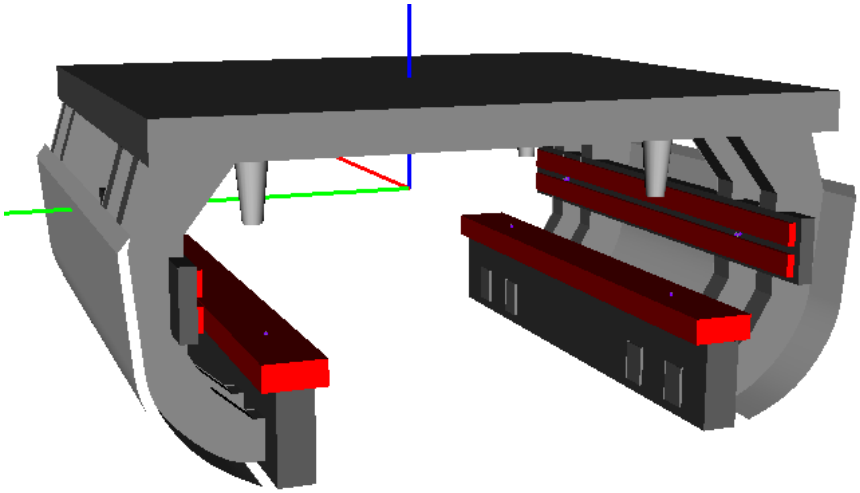

Figure 1.15. Model of maglev bogie

We consider two bogie models
{UM Data}\Samples\MagLev\Bogie_6DOF,
{UM Data}\Samples\MagLev\Bogie.
The model with 6 DOF is the most simple maglev model for testing main features of UM MagLev, and for comparison of simulation result with analytical ones. In this model the magnet holders are rigidly connected with a frame. In the second model the magnets have additional degrees of freedom, which correspond to the primary suspension of the maglev vehicle.

1.4.1.1. Frame

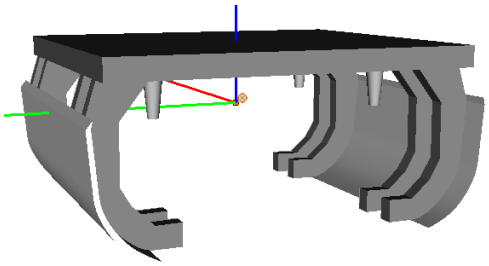

The frame body has 6 degrees of freedom, which are introduced by the joint jFrame. The inertial parameters are set by the identifiers

m_frame - mass

iframe_x, iframe_z, iframe_z - central moments of inertia relative to the X, Y, Z axis

z_cg_frame - vertical coordinate of the center of gravity.

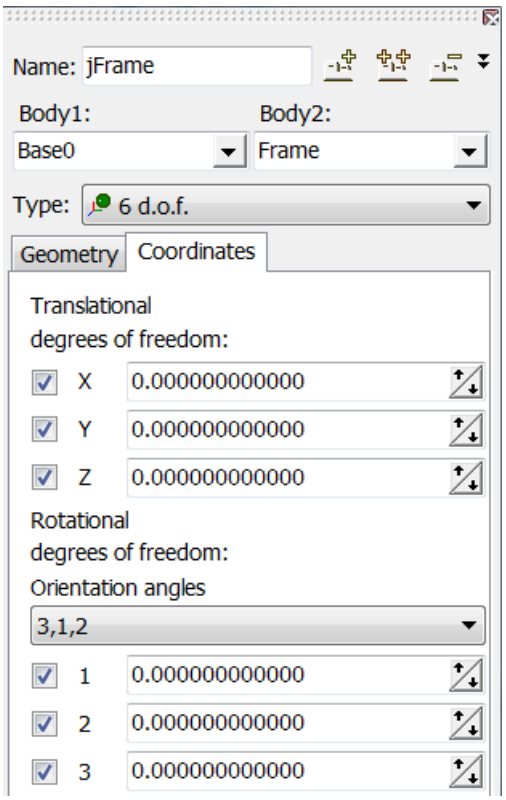

Figure 1.16. Six degrees of freedom for frame

1.4.1.2. Levitation magnets

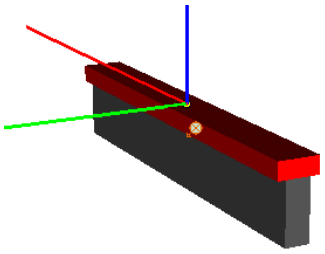

In the case of the **Bogie_6DOF** model, two levitation magnet holders **LMagnet L** (levitation magnet left), **LMagnet R** (levitation magnet right) are rigidly connected to the frame by the joints with zero degrees of freedom **jLMagnet L, jLMagnet R,** Figure 1.17**,** left. For the model **Bodie** with primary suspension, the levitation magnets have tree DOF**,** Figure 1.17**,** right.

Identifiers parameterize both geometric and inertia data:

m_magnet_l - mass

ix_magnet_l, iy_magnet_l, iz_magnet_l - central moments of inertia relative to the X, Y, Z axis

z_cg_magnet_l - vertical coordinate of the center of gravity

lmagnet_y, lmagnet_z - lateral and vertical position parameters

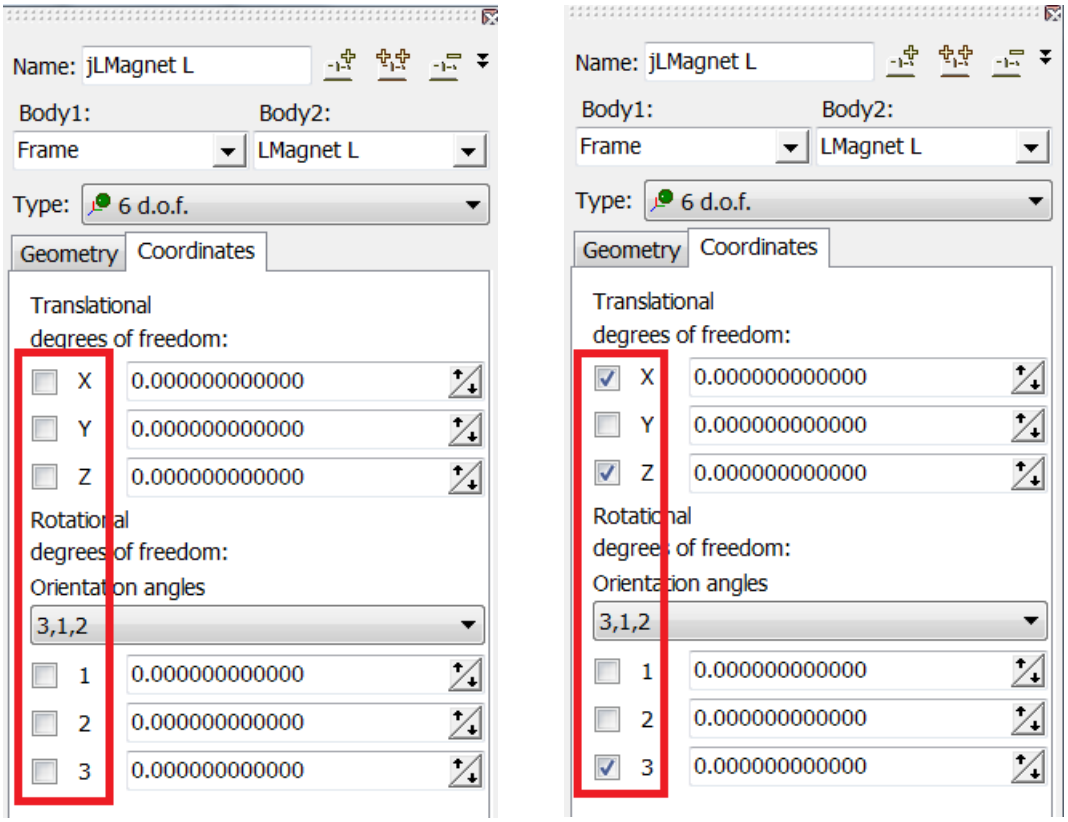

Figure 1.17. Rigid and 3 DOF coupling of levitation magnet

1.4.1.3. Guidance magnets

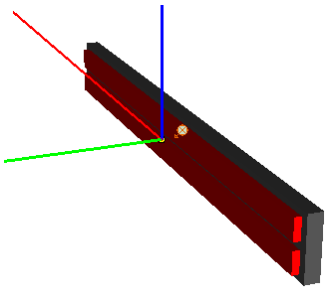

In the case of a bogie_6DOF model, two guidance magnet holders **GMagnet L** (guidance magnet left), **GMagnet R** (guidance magnet right) are rigidly connected to the frame by the joints with zero degrees of freedom **jGMagnet L, jGMagnet R,** Figure 1.18, left. For the model **Bodie** with primary suspension, the levitation magnets have tree DOF**,** Figure 1.18**,** right.

Identifiers parameterize both geometric and inertia data:

m_magnet_g - mass

ix_magnet_g, iy_magnet_g, iz_magnet_g - central moments of inertia relative to the X, Y, Z axis

z_cg_magnet_g - vertical coordinate of the center of gravity

gmagnet_y, gmagnet_z - lateral and vertical position parameters

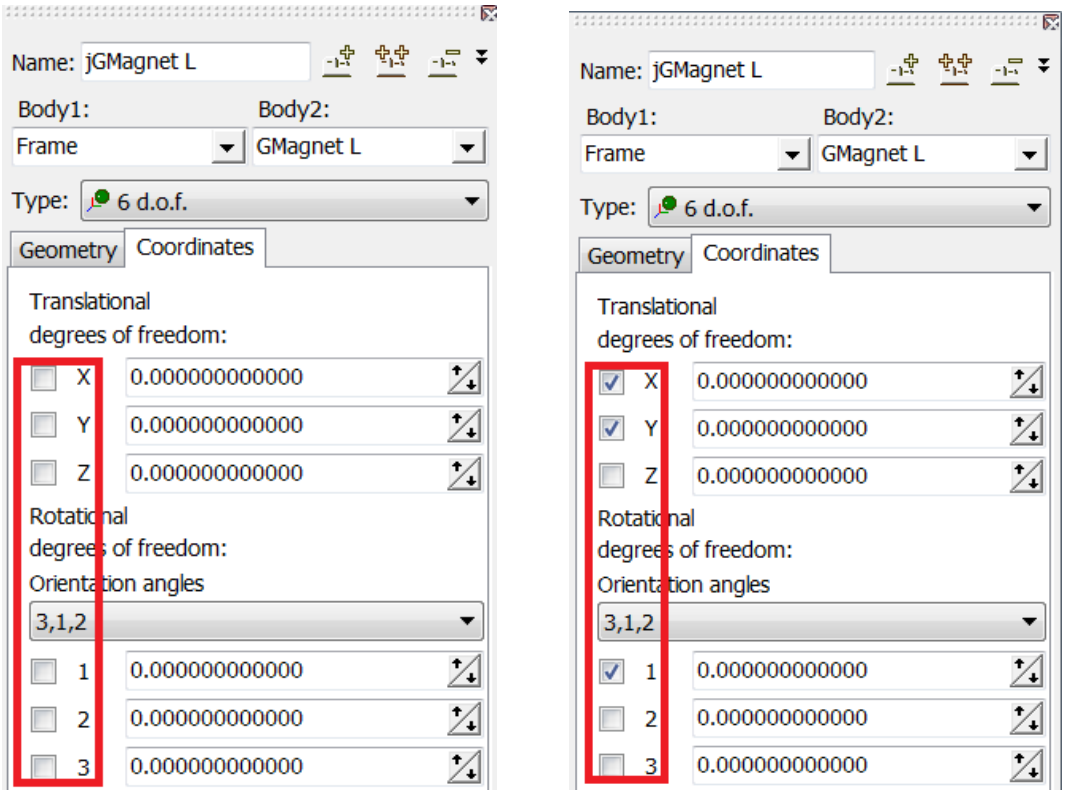

Figure 1.18. Rigid and 3 DOF coupling of guidance magnet

1.4.1.4. Sensors

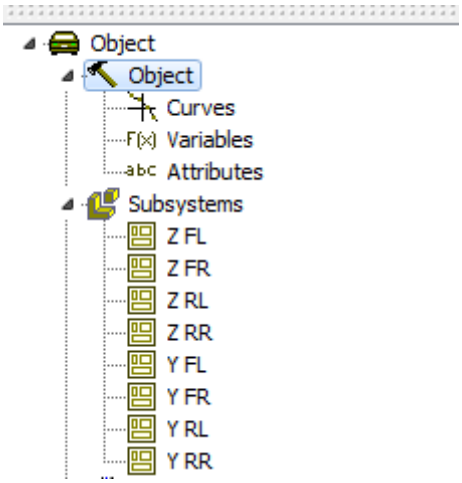

Figure 1.19. Accelerometers as included subsystems

The model contains a subsystem **Sensors** with 8 accelerometers for measuring magnet accelerations. Each of the accelerometers is added as an included subsystem, Figure 1.19.

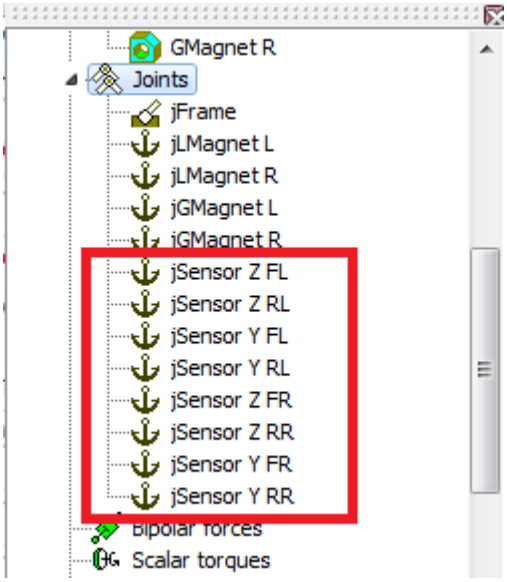

Figure 1.20. Joints for sensor positioning

Joints with zero degrees of freedom are used for positioning the accelerometers, Figure 1.20, Section 1.3.5 *Accelerometer positioning*.

1.4.1.5. Magnet forces

Two magnets are connected to each of the magnet holders.

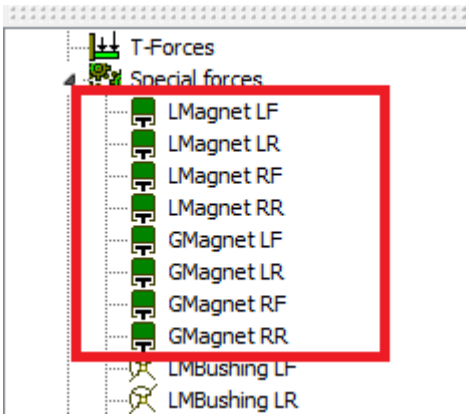

Figure 1.21. Magnet forces

Four levitation magnets are **LMagnet LF** (levitation magnet left front), **LMagnet LR** (levitation magnet left rear), **LMagnet RF**, **LMagnet RR**. Identifiers parameterizing the forces are

lmagnet_base - the lateral distance between the magnets

fz_lmagnet_lf, *fz_lmagnet_lr*, *fz_lmagnet_rf*, *fz_lmagnet_rr* – identifiers for external computation of levitation forces in Matlab/Simulink.

Four guidance magnets are **GMagnet LF** (guidance magnet left front), **GMagnet LR** (guidance magnet left rear), **GMagnet RF**, **GMagnet RR**. Identifiers parameterizing the forces are

gmagnet_base - the lateral distance between the magnets

fz_gmagnet_lf, *fz_gmagnet_lr*, *fz_gmagnet_rf*, *fz_gmagnet_rr* – identifiers for external computation of guidance forces in Matlab/Simulink.

Accelerometer data are assigned to each of the magnet force.

1.4.1.6. Primary suspension: Bushings

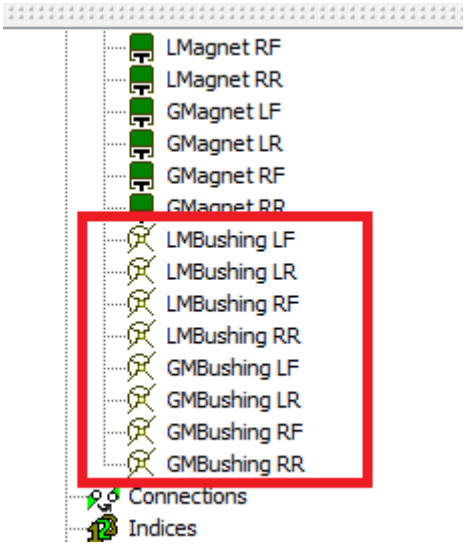

Figure 1.22. Magnet forces

The magnet holders are coupled with the frame by linear viscous-elastic bushings, which correspond to the *primary suspension* of the maglev vehicle. The bushings have no effect in the case of the model with 6 DOF, when the holders are rigidly connected with the frame by the joints. These elements are used in the model with primary suspension **Bogie**.

Spring and damper constants for the primary suspension are computed according to the frequency and damping ratio constants, which are set by the +identifiers *f_prim* and *beta_prim*, Figure 1.23.

Весь список | Control | Bushings

Name	Expression	Value	Comment
f_prim	7		Primary suspension: frequency (Hz)
beta_prim	0.4		Primary suspension: damping ratio
x_bush_l	1		Bushing longitudinal position (levitation)
z_bush_s	-0.8		Bushing vertical position (levitation)
k_bush_s	sqr(2*pi*f_prim)*m_magnet_l/2	5.8033274E+5	Bushing stiffness (levitation)
ka_bush_s	1.0000000E+5		Bushing angular stiffness (levitation)
c_bush_s	2*beta_prim*sqrt(k_bush_s*m_magnet_l)	1.4928087E+4	Bushing damping (levitation)
ca_bush_s	1000		Bushing angular damping (levitation)
x_bush_g	1		Bushing longitudinal position (guidance)
z_bush_g	-0.18		Bushing vertical position (guidance)
y_bush_g	1.6		Bushing lateral position (guidance)
k_bush_g	sqr(2*pi*f_prim)*m_magnet_g/2	5.8033274E+5	Bushing stiffness (guidance)
ka_bush_g	1.0000000E+5		Bushing angular stiffness (guidance)
c_bush_g	2*beta_prim*sqrt(k_bush_g*m_magnet_g)	1.4928087E+4	Bushing damping (guidance)
ca_bush_g	1000		Bushing angular damping (guidance)

Figure 1.23. Parameterization of primary suspension

1.4.1.7. Sliding contact elements

The bogie model includes a sliding contact force element **Upper contact**, which allows the equilibrium positioning of the bogie in case of disable levitation magnets as well as the vehicle landing on the track in emergency cases, Figure 1.24-Figure 1.26.

The element contains four contact points. The gap is parameterized by the identifier *s0_contact*, Figure 1.26.

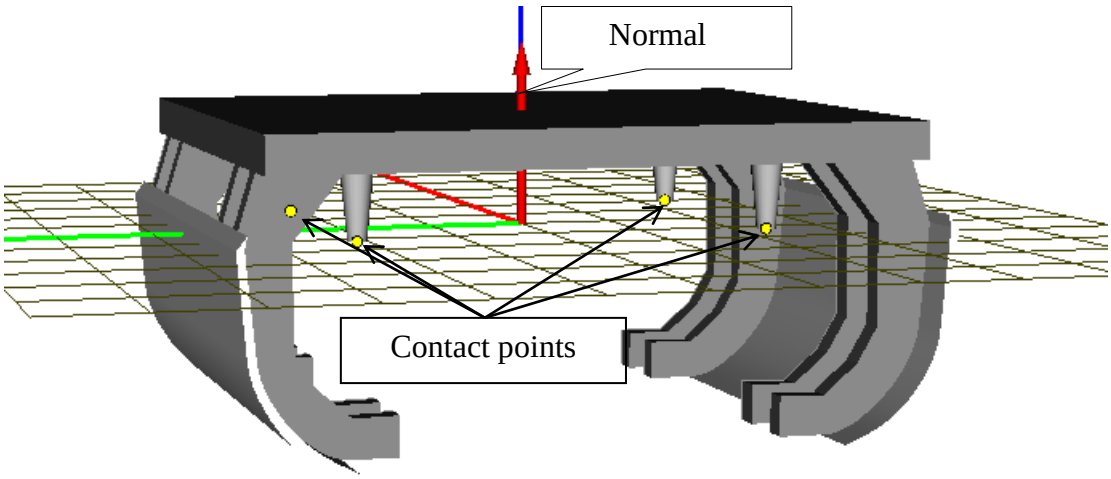

Figure 1.24. Sliding contact

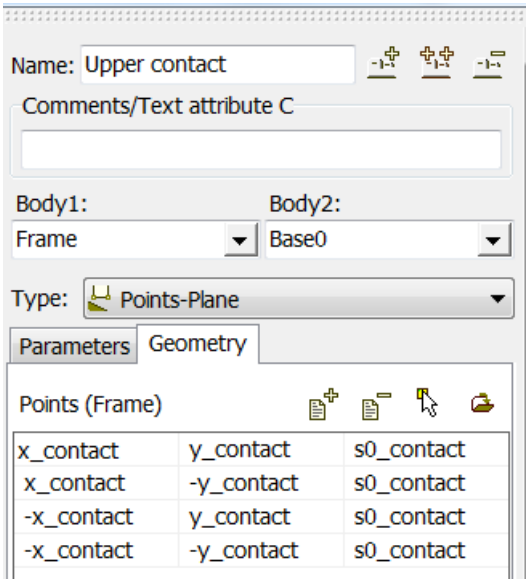

Figure 1.25. Contact points

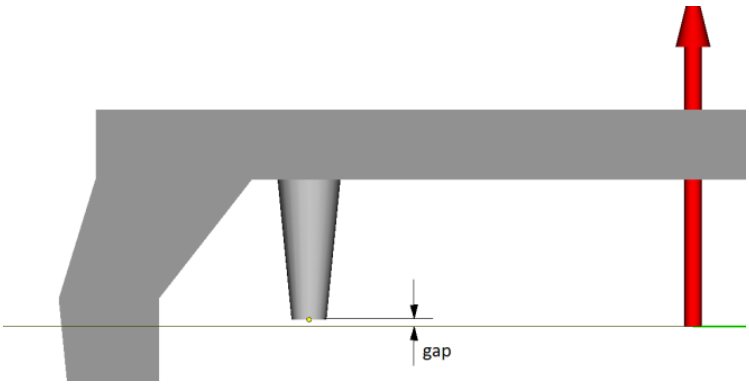

Figure 1.26. Gap between contact points and contact plane

1.4.1.8. Identifiers for magnet control

The model includes a list of identifiers, which are necessary for parameterization of magnet control parameters. The parameterization is used in linear analysis of maglev vehicles as well in multivariant computations. It allows the user to analyze the levitation properties in dependence on the control parameters.

Whole list | Control | Bushings | Inertia | Geometry | Contact | Magnet force identifiers

Name	Expression	Value	Comment
Ul_0	0		Stationary voltage (levitation)
Ul_s	0		Proportional control (levitation)
Ul_v	0		Differential control (levitation)
Ul_a	0		Acceleration control (levitation)
Ul_is	0		Integral control (levitation)
Ug_0	0		Stationary voltage (guidance)
Ug_s	0		Proportional control (guidance)
Ug_v	0		Differential control (guidance)
Ug_a	0		Acceleration control (guidance)
Ug_is	0		Integral control (guidance)
Fz0	m_control*9.81/1000	10.791	Nominal control force (kN)
Fy0	0		Stationary force (guidance)
s0_l	10		Levitation: nominal gap (mm)
s0_g	10		Guidance: nominal gap (mm)

Figure 1.27. Parameterization of control parameters

1.4.2. Bogie model with U-shaped magnets

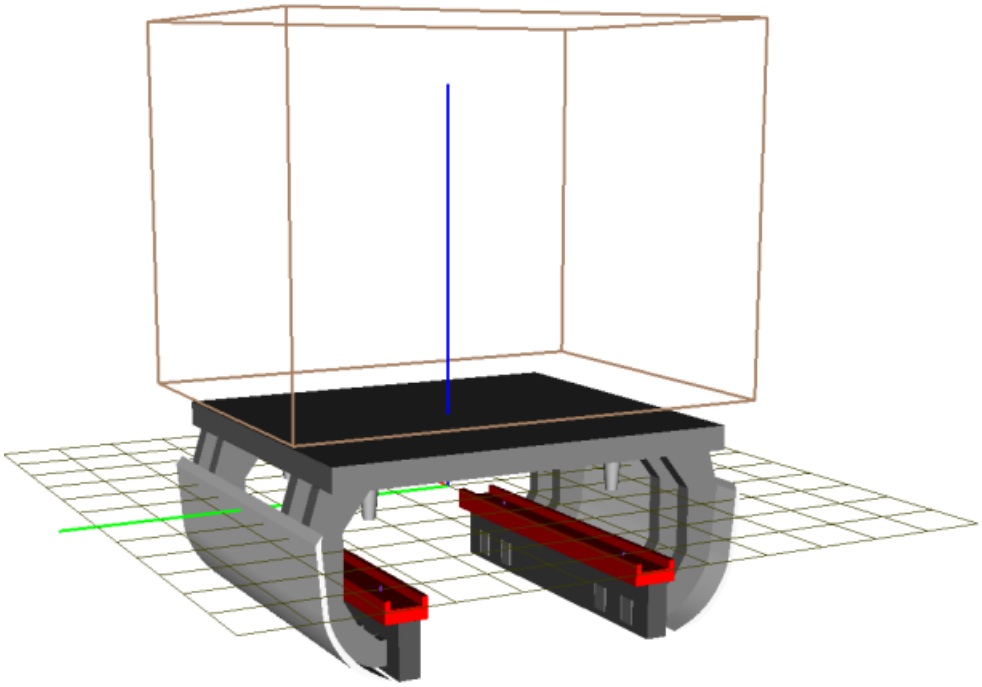

Figure 1.28. Model for tests of U-shaped magnets

The model illustrates a passive guidance maglev system, see Section 1.6.3 U-shaped magnet. It is located in the directory

{UM Data}\Samples\MagLev\MagLev vehicle

The model is based on the previous bogie model with some changes:

- guidance magnets are excluded;
- a car body reduced to one bogie is added;
- the Suspension bushing describes a simple linear secondary suspension;
- the identifier *lambda_ratio* is added for parameterization of the lateral force ratio, Section

1.5. Track macro profile and roughness

Guideway geometry is composed of two components: macro profile, and roughness.

1.5.1. Track macro profile

Track macro profile contains 3D information about the geometry of the centerline on the top of track beam. More information about the monorail track geometry can be found in the file Chapter 26.

1.5.2. Track roughness (irregularities)

Development of track roughness (irregularities) files *.irr is described in details in Chapter 12 file, Sect. *Micro profile (irregularities)*.

Here we consider some features related to maglev systems.

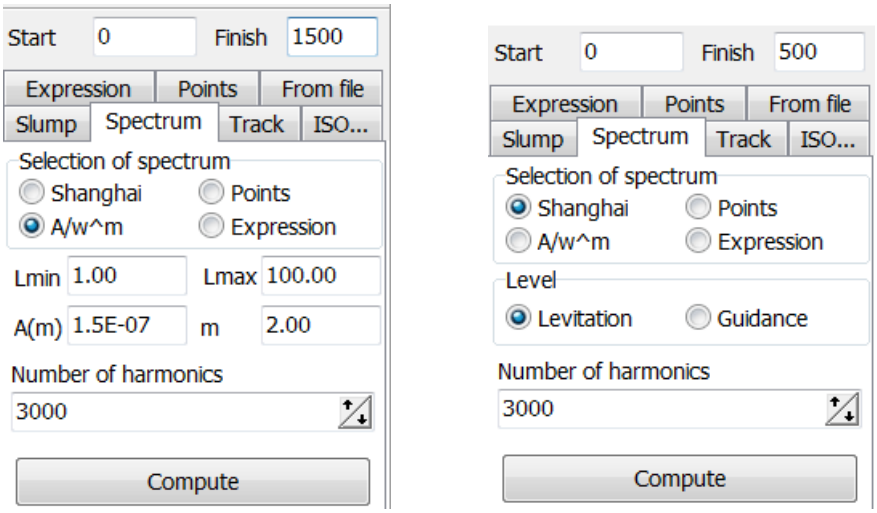

Figure 1.29. Variants of PSD for maglev track roughness

Roughness files for maglev track are generated in the tool available in the UM Simulation by the **Tools | Irregularity editor…| Monorail track** main menu command. The irregularities are generated by standard power spectral density (PSD) function, Figure 1.29.

The following PSD function is considered in [1], [2], [3]

$$S(\Omega)=\frac{A_s}{\Omega^2},\ \Omega=\frac{2\pi}{\lambda}$$

where Ω is the wave number, λ is the wave length in meters, A_s is the roughness parameter or amplitude, Figure 1.29, left . For a very smooth guideway, the roughness parameter may be assumed to be $A_s=1.5e^{-7}$ m [1], Figure 1.30, top.

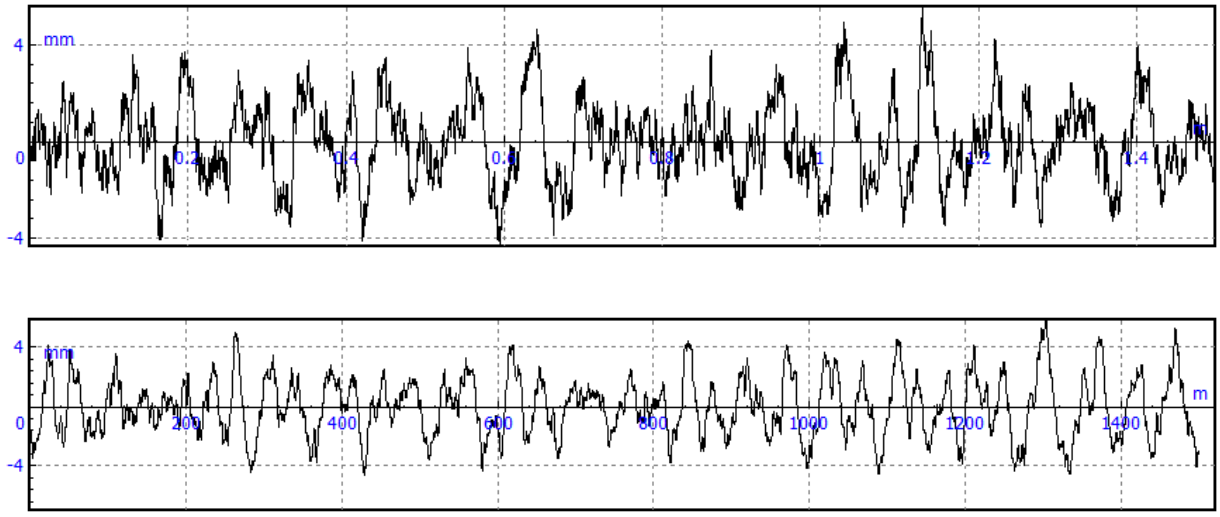

Figure 1.30. Generated roughness curves

The following PSD function

$$S(\Omega) = \frac{A(\Omega^2 + B\Omega^3 + C)}{\Omega^4 + D\Omega^3 + E\Omega^2 + F\Omega + G}$$

is considered in paper [4] for the Shanghai Maglev track basing on analysis of measurements. The parameters A-G proposed in this paper are implemented as 'Shanghai' spectrum both for the levitation and guidance track level, Figure 1.29, right. An example of the generated roughness on the levitation level is sown in Figure 1.30, bottom.

Four irregularities files can be assigned as track roughness data (Figure 1.31)

- **Levitation level (left, right)**
- **Guidance level (left, right)**

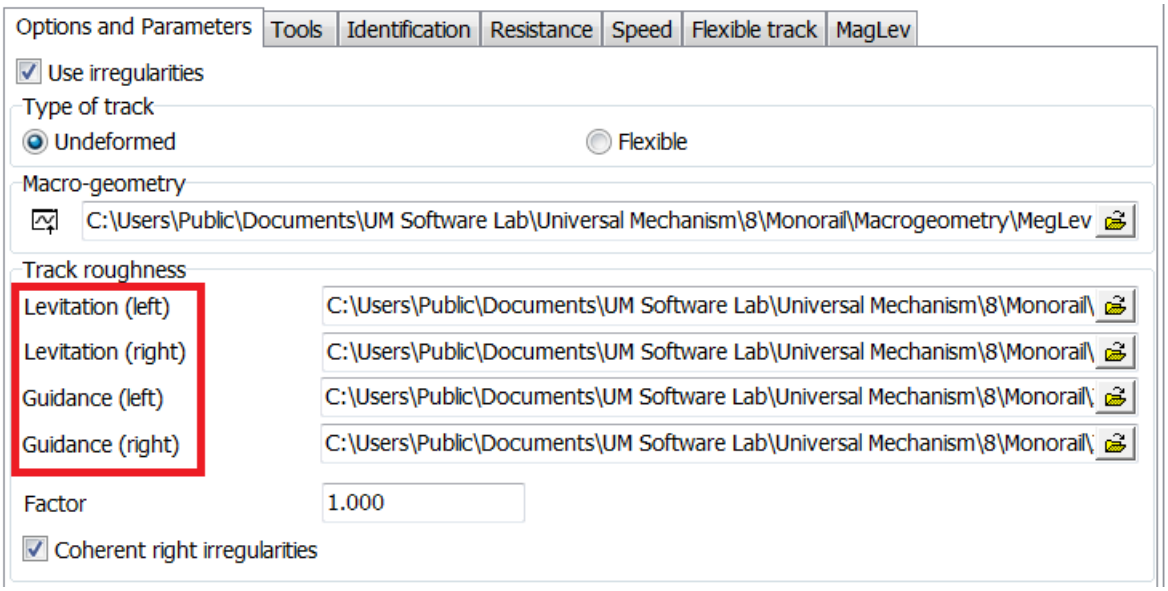

Figure 1.31. Track roughness files

Information about other parameters of the track roughness can be found in the file Chapter 26.

1.6. Magnet models

In this section we consider models of levitation and guidance magnets for simulation of EMS maglev vehicles.

1.6.1. Spring-damper model

A spring-damper model of a magnet is the simplest one. It does not take into account the controller effects, but sometimes this model is useful, [5], [6]. In particular, such model is recommended to be used for evaluation of natural frequencies of UM maglev models.

The linear model produces the magnet force

$$F = F_0 + k_p(S - S_0) + c_p\dot{S},$$

where F_0 is the nominal magnet force, S_0 is the nominal gap, S is the current gap value, and k_p, c_p are the spring and damper constants.

1.6.2. Single pole magnet model

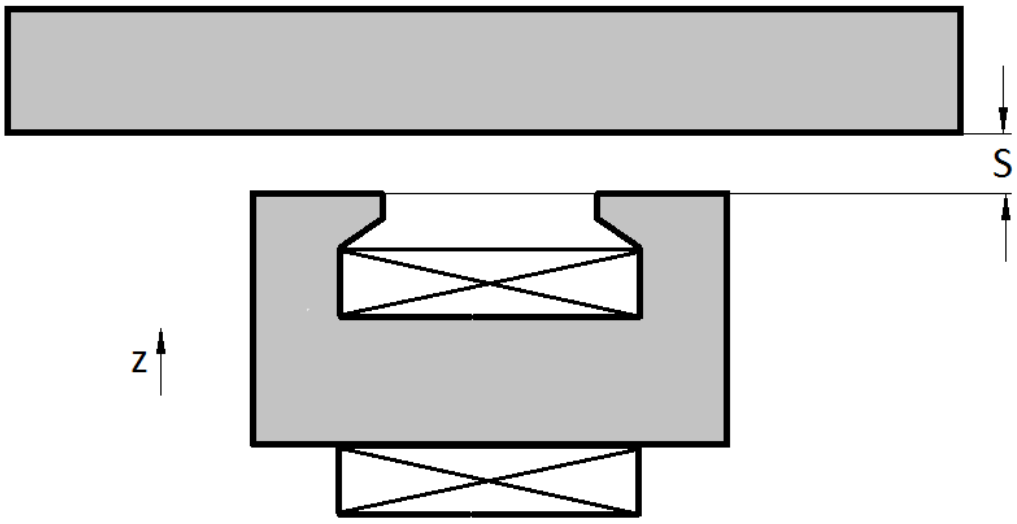

Figure 1.32. Magnet

A single pole magnet model is the most frequently used in maglev simulation; see e.g. [7], [8], [9], [10], [11], [12].

The electromagnet force is computed according to the formula

$$F = \kappa\left(\frac{I}{S}\right)^2, \tag{1.1}$$

where I is the current, S is the magnet gap, and κ is the magnet constant

$$\kappa = \frac{\mu_0 A N^2}{4}.$$

Here A is the area of the magnet pole, N is the number of magnet coil turns, and μ_0 is the permeability of vacuum.

The single pole magnet model includes the voltage equation

$$\frac{d(LI)}{dt} = -RI + U,$$

where R is the resistance, U is the voltage, and L is the inductance depending on the gap S and the magnet constant κ

$$L = \frac{2\kappa}{S}.$$

Then,

$$L\dot{I} = -RI + \frac{LI}{S}\dot{S} + U\ .$$

Consider first a stationary state of the magnet model. Let F_0, S_0 be the nominal magnet force and gap. Then the stationary values of other variables are

$$I_0 = S_0\sqrt{F_0/\kappa},$$

$$U_0 = RI_0,$$

$$L_0 = \frac{2\kappa}{S_0}$$

The magnet control model considered in this section is

$$U = U^0 + U_s\Delta S + U_v\dot{S} + U_{is}\int_0^t \Delta S dt - U_a\ddot{Z}\ .$$

$$\Delta S = S - S_0$$

The vertical magnet coordinate Z is opposite in direction to the gap S, Figure 1.32. If the integral part of the control model is not presented, i.e. $U_{is} = 0$, then the initial voltage value is equal to the nominal one $U^0 = U_0 = RI_0$.

Taking into account the control model, the final voltage equation is

$$L\dot{I} = -RI + U^0 + U_s\Delta S + (U_v + LI/S)\dot{S} + U_{is}\int_0^t \Delta S dt - U_a\ddot{Z}\ .$$

Thus, the list of parameters describing the magnet model is

$$F_0, S_0, \kappa, R, U^0, U_s, U_v, U_{is}, U_a\ .$$

This model is applied both to the levitation and guidance magnets with different lists of magnet and control parameters.

1.6.3. U-shaped magnet

U-shaped magnets produce lateral forces, which can be used for passive guidance in cases of low and medium speed maglev systems. In addition to the axial attractive force, such magnets produce a side force. We consider two different models of U-shaped magnets, Models A and B.

Model A. The approximate force Model A of the U-core magnet was derived in [13] and used by many authors in maglev systems research [14], [15], [16].

According to [13], the axial (levitation) F_z and lateral F_y forces are

$$F_z = F\left(1+\frac{2S}{\pi W_m}-\frac{2y}{\pi W_m}\arctan\frac{y}{S}\right),$$

$$F_y = F\frac{2S}{\pi W_m}\arctan\frac{y}{S},$$

where F is the force value according to Eq. (1.1), y is the lateral shift of the magnet, and W_m is the pole width.

Let us introduce the lateral force ratio

$$\lambda_{\mathrm{A}} = \frac{2S_0}{\pi W_m}.$$

Then the final expressions for the U-shaped magnet Model A are as follows:

$$\begin{aligned} F_z &= F\left(1+\lambda_{\mathrm{A}}\frac{S}{S_0}-\lambda_{\mathrm{A}}\frac{y}{S_0}\arctan\frac{y}{S}\right) = F\left(1+\lambda_{\mathrm{A}}\frac{S}{S_0}\right)-F_y\frac{y}{S}, \\ F_y &= F\lambda_{\mathrm{A}}\frac{S}{S_0}\arctan\frac{y}{S} = F\psi_{\mathrm{A}}(y,S,S_0). \end{aligned} \qquad (1.2)$$

If $\lambda_{\mathrm{A}}=0$, the model (1.2) exactly corresponds to the magnet model (1.1).

Model B. The next model was proposed in [17]. Using the above designations, the levitation F_z and lateral F_y forces are computed according to the formulas

$$F_z = \frac{1}{4}N^2\mu_0\left[\frac{(W_m-y)}{S^2}+\frac{4y}{4S^2+\pi Sy}\right]lI^2 = \frac{1}{4}N^2\mu_0 lW_m\left(\frac{I}{S}\right)^2-F_y\frac{y}{S},$$

$$F_y = \frac{1}{4}N^2\mu_0\left[\frac{1}{S}-\frac{4}{4S+\pi y}\right]lI^2 = \frac{1}{4}N^2\mu_0 lW_m\left(\frac{I}{S}\right)^2\frac{\pi S_0}{4W_m}\frac{1}{(1+\pi y/(4S))}\frac{y}{S_0},$$

where l is the length of magnet.

Taking into account that $A = lW_m$ and introducing the lateral force ratio

$$\lambda_{\mathrm{B}} = \frac{\pi S_0}{4W_m} = \frac{\pi^2}{8}\lambda_{\mathrm{A}} = 1.234\lambda_{\mathrm{A}},$$

we obtain

$$F_z = F\left[1-\lambda_B \frac{1}{(1+\pi y/(4S)}\frac{y}{S_0}\frac{y}{S}\right] = F - F_y\frac{y}{S},$$
$$F_y = F\lambda_B \frac{1}{(1+\pi y/(4S))}\frac{y}{S_0} = F\psi_B(y,S,S_0) \qquad (1.3)$$

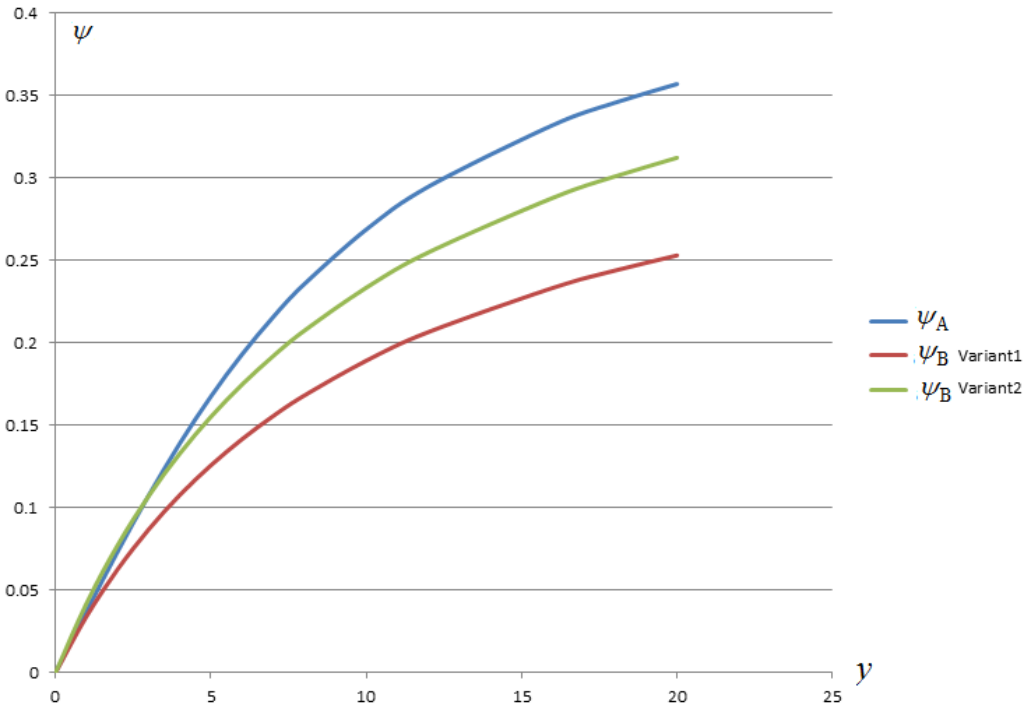

Figure 1.33. Comparison of Models A,B

To compare Models A, B, consider plots of functions ψ_A, ψ_B versus lateral shift y in Figure 1.33. The functions are computed for $S = S_0 = 8\text{mm}$, $\lambda_A = 0.3$ and $\lambda_B = \lambda_A$ (Variant 1) or $\lambda_B = 1.234\lambda_A$ (Variant 2). For small lateral shift Variant 2 gives a good correlation of Models A and B.

The user should select one of the Models A or B and set a value of the lateral force ratio λ in UM simulation program before simulation start, Figure 1.34, Section 1.8.2 Maglev control parameters.

It is allowed modeling staggered configuration of U-shaped levitation magnets, 1.8.3 *Staggered configuration of U-core levitation magnets*.

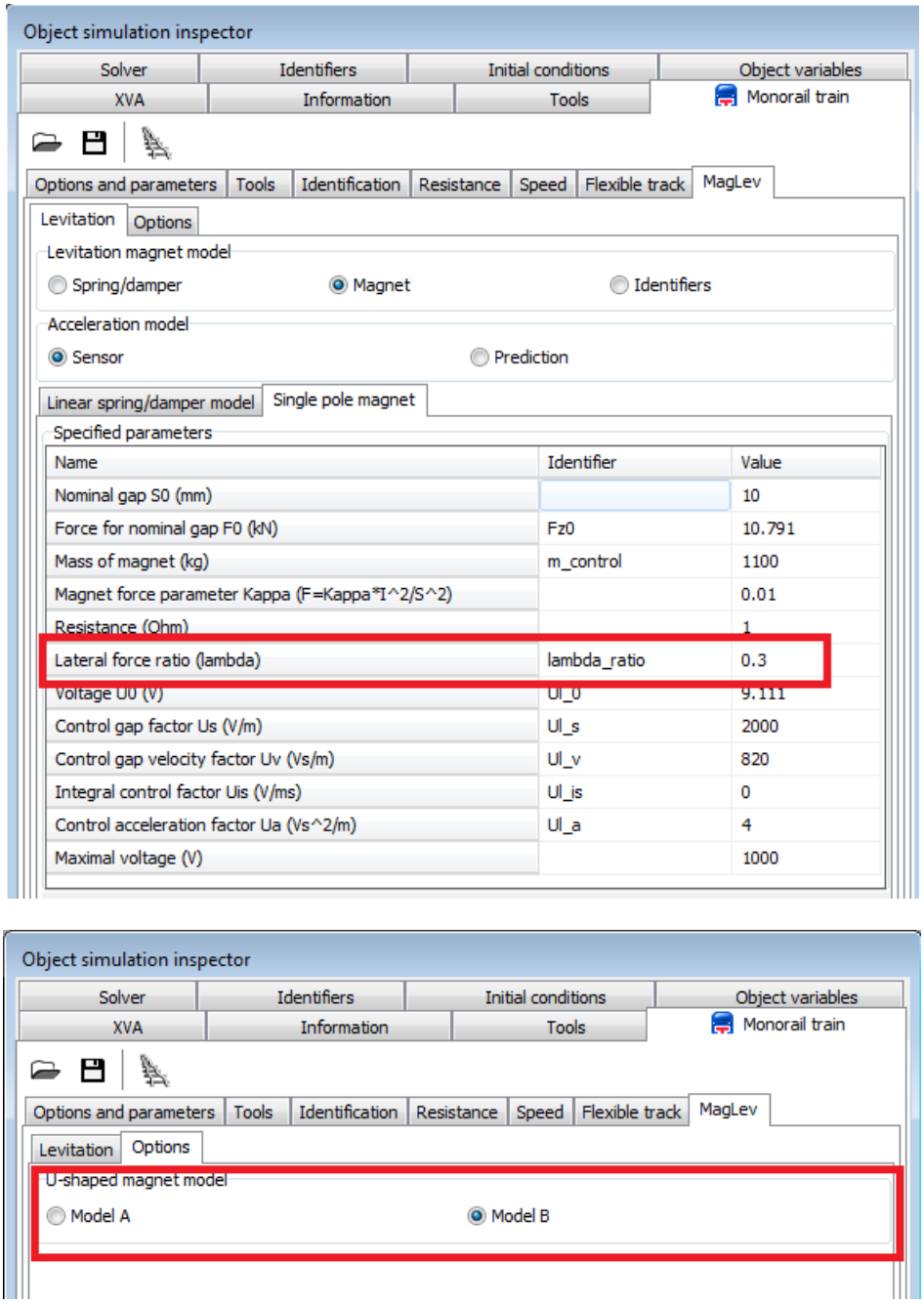

Figure 1.34. Specifying U-shaped magnet model

1.6.4. External magnet models

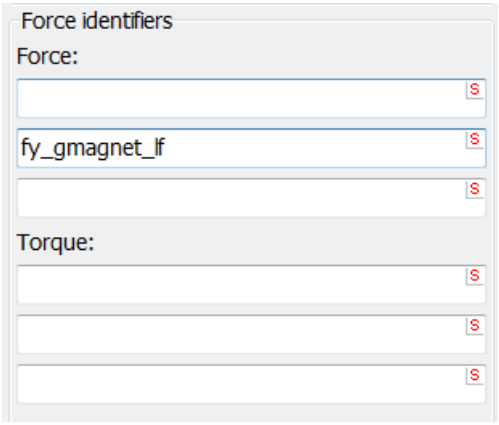

Figure 1.35. Parameterization of force for guidance magnet

The user may develop own models of magnets. User's models are based on programming identifiers, which parameterize force and torque acting on the magnet, Section 1.3.2 *Modeling levitation and guidance magnets*.

The identifiers correspond to the force and torque components in the track system of coordinates (TSC), Figure 1.35. The origin of TSC coincides with the projection of the magnet point on the ideal central axis of the track; the X axis coincides with the track tangent, the Y axis lies in the track plane on the left to the motion direction, and the Z axis is directed upwards.

Remark. According to this description of force components, guidance forces for the left and right guidance magnets must differ in sign4 the force is positive for the right magnet and negative for the left one. The user should remember that if he rotates about a vertical axis on 180 degrees a subsystem with magnets, the guiding forces change their signs.

The force models are constructed with use of UM variables corresponding gaps, their time derivatives and integrals, Section 1.8.6.2 *Gap*, as well as the variables corresponding to the model identifiers and so on.

The following tools and modules van be used for programming identifiers:

Identifier control

The tool allows develop very simple models such as a spring-damper one. This method is use for test of the identifiers programming only; it cannot be applied in complex cases, see Section 1.10.4 *Spring/damper magnet model as identifier control*.

Block editor

See Chapter 24 for development of model with the Block editor tool.

Interface to Matlab/Simulink

See the gs_um_control.pdf file to get information about the development of force models in Matlab/Simulink

Programming in control file

Theoretically the forces of any complexity can be computed in the Control file, see Chapter 5.

1.6.5. Theoretical results on stability

Consider a one degree model of a magnetic suspension to get basic results on stability of electromagnetic suspension. The model is shown in Figure 1.32. The 1 d.o.f. model of the controlled magnet is described by two equations

$$m\ddot{Z} = -F_0 + \kappa\left(\frac{I}{S}\right)^2$$

$$L\dot{I} = -RI + U_0 + U_s\Delta S + (U_v + LI/S)\dot{S} - U_a\ddot{Z}$$

Here m is the magnet mass. The integral control is not considered.

Let us introduce dimensionless variables

$$i = \frac{I - I_0}{I_0}, s = \frac{S - S_0}{S_0} = -\frac{Z - Z_0}{S_0}$$

$$mS_0\ddot{s} = F_0 - \kappa\left(\frac{I_0}{S_0}\right)^2\left(\frac{1+i}{1+s}\right)^2 = -F_0\left(\frac{1+i}{1+s}\right)^2 + F_0,$$

$$\frac{L_0 I_0}{1+s}\dot{i} = -RI_0(1+i) + U_0 + U_s S_0 s + (U_v S_0 + LI_0/(1+s))\dot{s} + U_a S_0\ddot{s}.$$

Suggesting that the variables *s*, *i* are small, the linearization of equation gives

$$\frac{mS_0}{2F_0}\ddot{s} = s - i,$$

$$\frac{L_0}{R}\dot{i} = -i + \frac{U_s S_0}{U_0}s + \left(\frac{U_v S_0}{U_0} + \frac{L_0}{R}\right)\dot{s} + \frac{U_a S_0}{U_0}\ddot{s}.$$

Now we introduce two time constants

$$T = \sqrt{\frac{mS_0}{2F_0}}, T_i = \frac{L_0}{R}$$

and dimensionless control parameters

$$k_s = \frac{U_s S_0}{U_0}, k_v = \frac{U_v S_0}{U_0 T}, k_a = \frac{U_a S_0}{U_0 T^2}.$$

Finally, the linearized electromagnet equations for stability analysis looks like

$$T^2\ddot{s} = s - i,$$

$$T_i\dot{i} = -i + k_s s + (k_v T + T_i)\dot{s} + k_a T^2\ddot{s}.$$

Searching the solution of this equations as

$$s = c_s e^{\lambda t}, i = c_i e^{\lambda t}$$

leads to the matrix equation

$$\begin{pmatrix} T^2\lambda^2 - 1 & 1 \\ -k_a T^2\lambda^2 - (k_v T + T_i)\lambda - k_s & T_i\lambda + 1 \end{pmatrix}\begin{pmatrix} c_s \\ c_i \end{pmatrix} = 0$$

The determinant of the matrix must be zero, so the characteristic equation is

$$\det\begin{pmatrix} T^2\lambda^2 - 1 & 1 \\ -k_a T^2\lambda^2 - (k_v T + T_i)\lambda - k_s & T_i\lambda + 1 \end{pmatrix} = 0,$$

$$T^2 T_i \lambda^3 + T^2(1+k_a)\lambda^2 + k_v T\lambda + k_s - 1 = 0,$$

$$a_0 = T^2 T_i,\ a_1 = T^2(1+k_a),\ a_2 = k_v T,\ a_3 = k_s - 1.$$

The Hurwitz matrix

$$\begin{pmatrix} a_1 & a_3 & 0 \\ a_0 & a_2 & 0 \\ 0 & a_1 & a_3 \end{pmatrix}$$

gives the stability conditions

$$a_1 a_2 - a_0 a_3 > 0,\ a_3 > 0$$

or

$$k_s > 1,\ k_v > \frac{T_i(k_s - 1)}{T(1+k_a)} = k_v^*, k_a > -1.$$

The stability conditions for the initial control parameters are

$$U_s > U_s^* = \frac{U_0}{S_0},\ U_v > U_v^* = \frac{U_0 T k_v^*}{S_0},\ U_a > -U_a^*,\ U_a^* = \frac{U_0 T^2}{S_0}.$$

According to this result, the stable levitation requires both proportional and differential control. Increase of the proportional control factor U_s requires increased value of the differential control parameter U_v. In contrary, the use of acceleration control $U_a > 0$ allows decreasing the differential control factor U_v.

1.7. Track models

In UM, three types of monorail track models can be applied: an **undeformed** or **rigid track,** a **flexible beam** one and use of **FEM subsystems** for dynamic simulation of track parts. Detailed information about the track models can be found in the file Chapter 26.

1.7.1. Use of FEM subsystem for simulation of track parts

Creation of a FEM subsystem for dynamic simulation of a monorail track is described in Chapter 26, item “Simulation of track as FEM subsystem”. Among other things, that chapter shows how macro profile of track can be specified using nodes of the FEM subsystem.

In this chapter, let us consider some features of simulation of interactions of maglev train with the subsystems.

As opposed to the wheel monorail vehicle, maglev bogie does not contact with the track; it slides over the track surface with some gap. In a UM model, its value can exceed 0.2 m (particularly, if some parts of the magnet construction are ignored in the model), Figure 1.36.

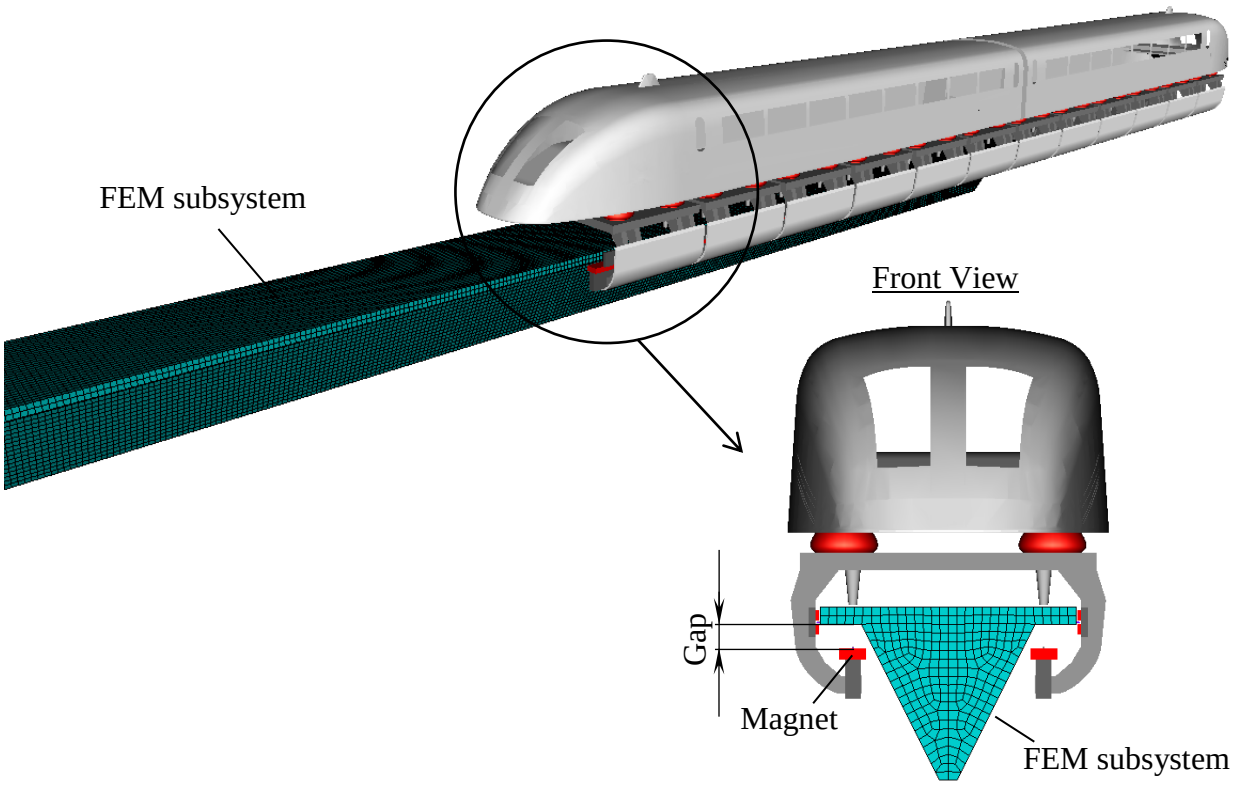

Figure 1.36. Gap between magnet of maglev train bogie and surface of FEM subsystem

Therefore, the tab sheets **Monorail track | General** differ for wheel and maglev monorail track subsystem. For maglev, the tab contain checkbox **Control gap** and field **Gap** to set gap value (see Figure 1.37). These controls are absent for wheel track but check box **Simulation of entry on edge** is added (see Figure 1.38).

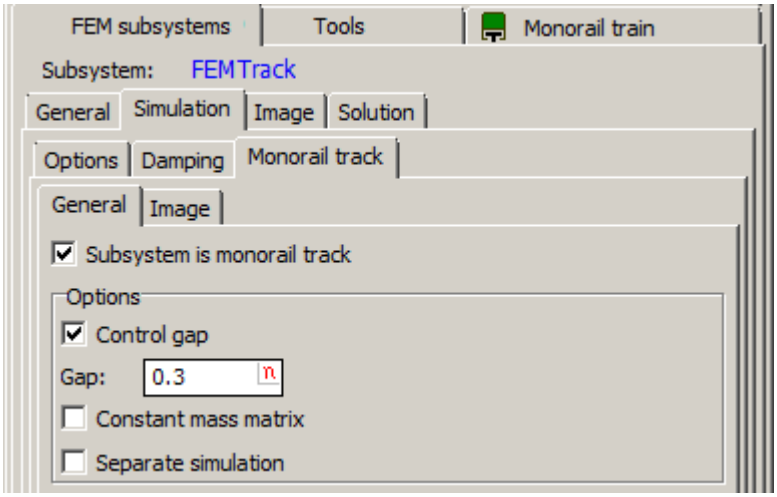

Figure 1.37. Tab sheet **Monorail track | General** for maglev monorail track subsystem

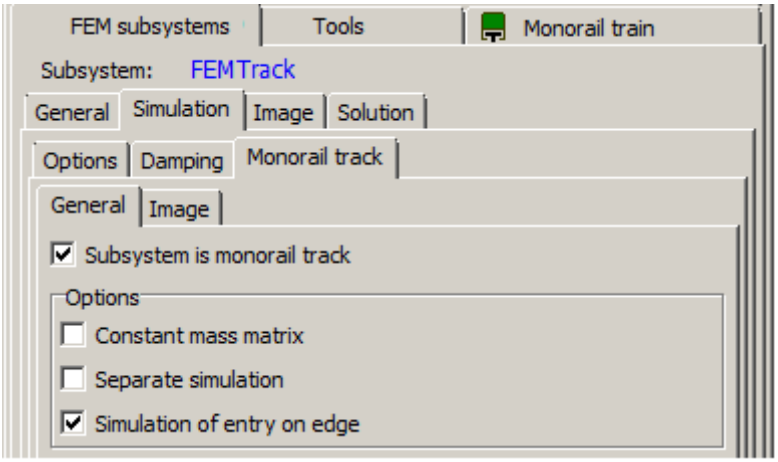

Figure 1.38. Tab sheet **Monorail track | General** for wheel monorail track subsystem

1.7.2. FEM track variables

All types of variables used for analysis of FEM subsystem can be applied for FEM track. In addition, the variables calculating track displacements under magnets are supported (see item 1.8.6.6).

1.7.3. Example

The example of simulation of flexible track parts of maglev monorail is available in site www.universalmechanism.com by link um_samples_fem_maglev_monorail.zip.

The FEM subsystem simulates the curvilinear part of the monorail track with constant radius 100 meters (see Figure 1.39 and Figure 1.40). General view and some parameters of the FEM subsystem are presented in Figure 1.41.

In Figure 1.42, the displacements under the front magnets and in the middle of the spans of the flexible track part are shown.

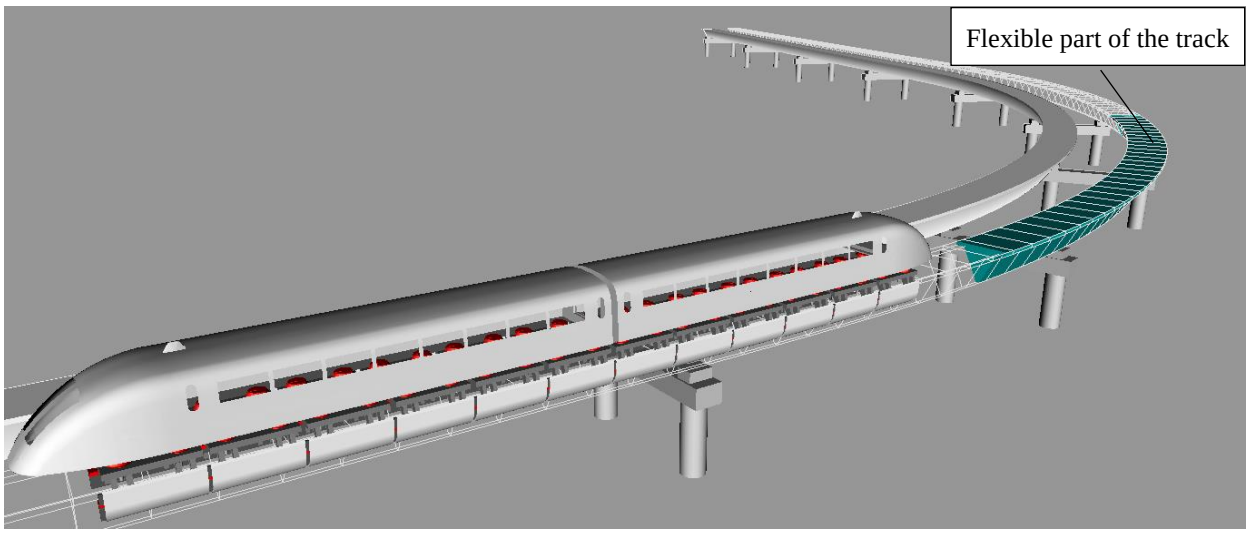

Figure 1.39. General view of the model from the example

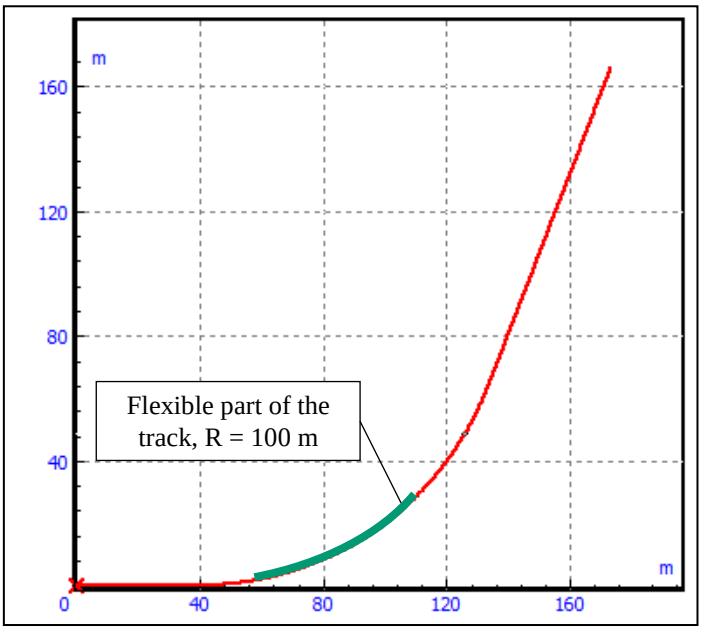

Figure 1.40. Horizontal macro profile of the track in the example

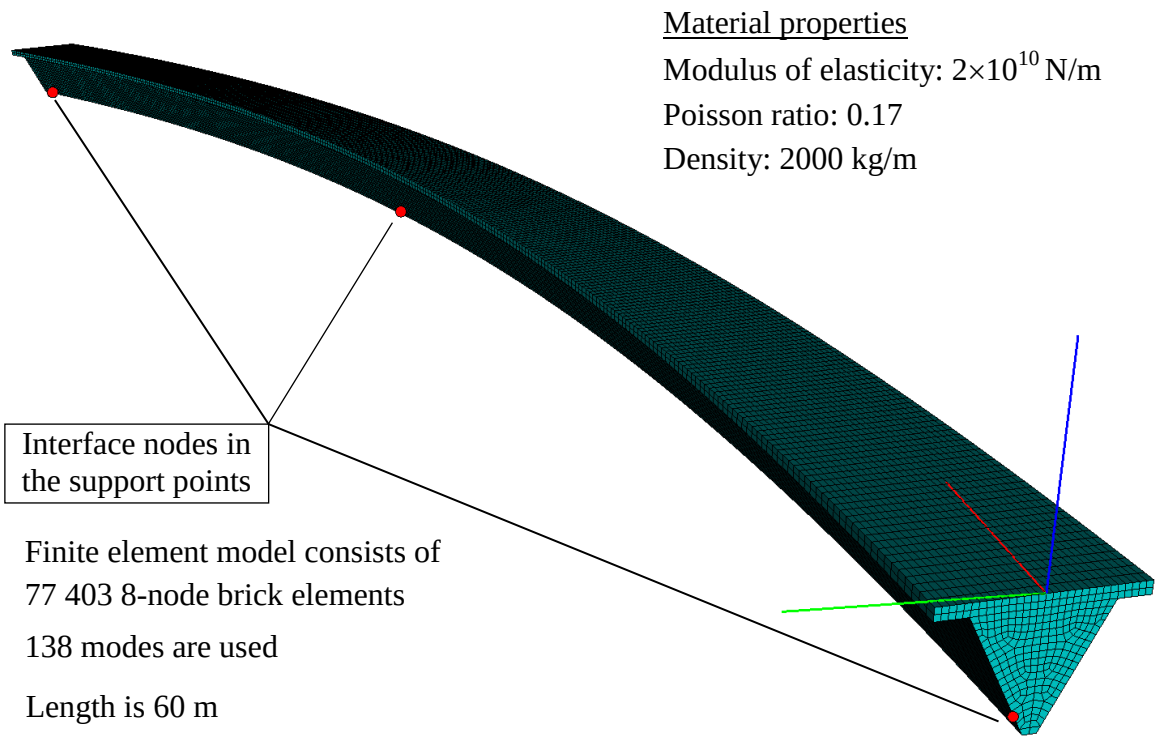

Figure 1.41. FEM subsystem simulating curvilinear part of the track in the example

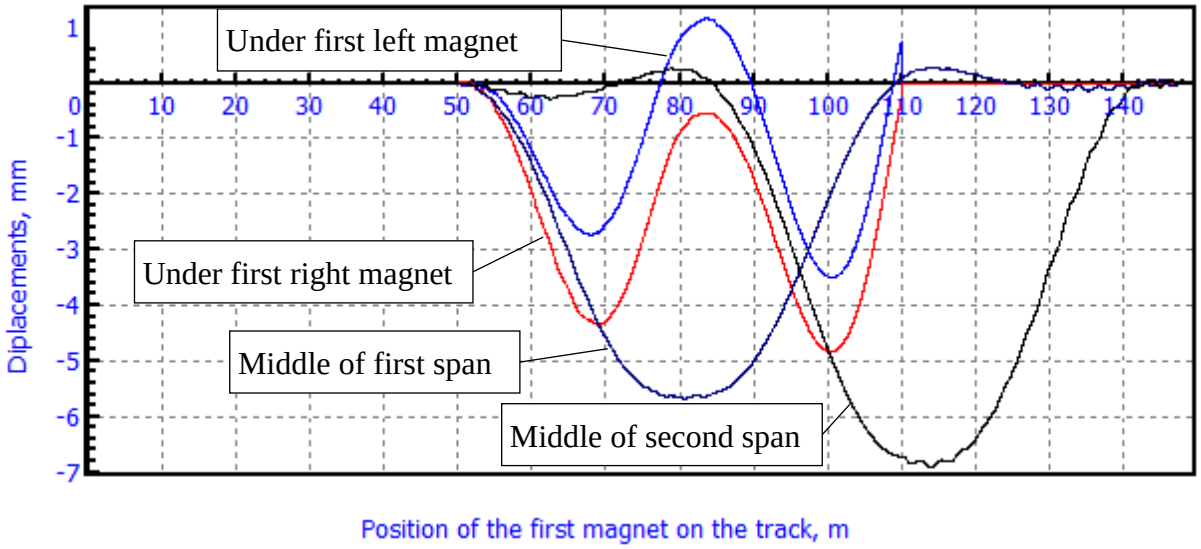

Figure 1.42. Displacements of the FEM part of the track

1.8. Simulation of maglev dynamics

In case of maglev systems, many of simulation parameters are similar to that for the monorail trains, see Chapter 26. The following sections there are useful for simulation of maglev trains:

Identification of longitudinal velocity control

Creating longitudinal velocity functions

Creating beam section profile

Modes of longitudinal motion of monorail

Kinematic characteristics relative to track system of coordinates

1.8.1. Preparing for simulation

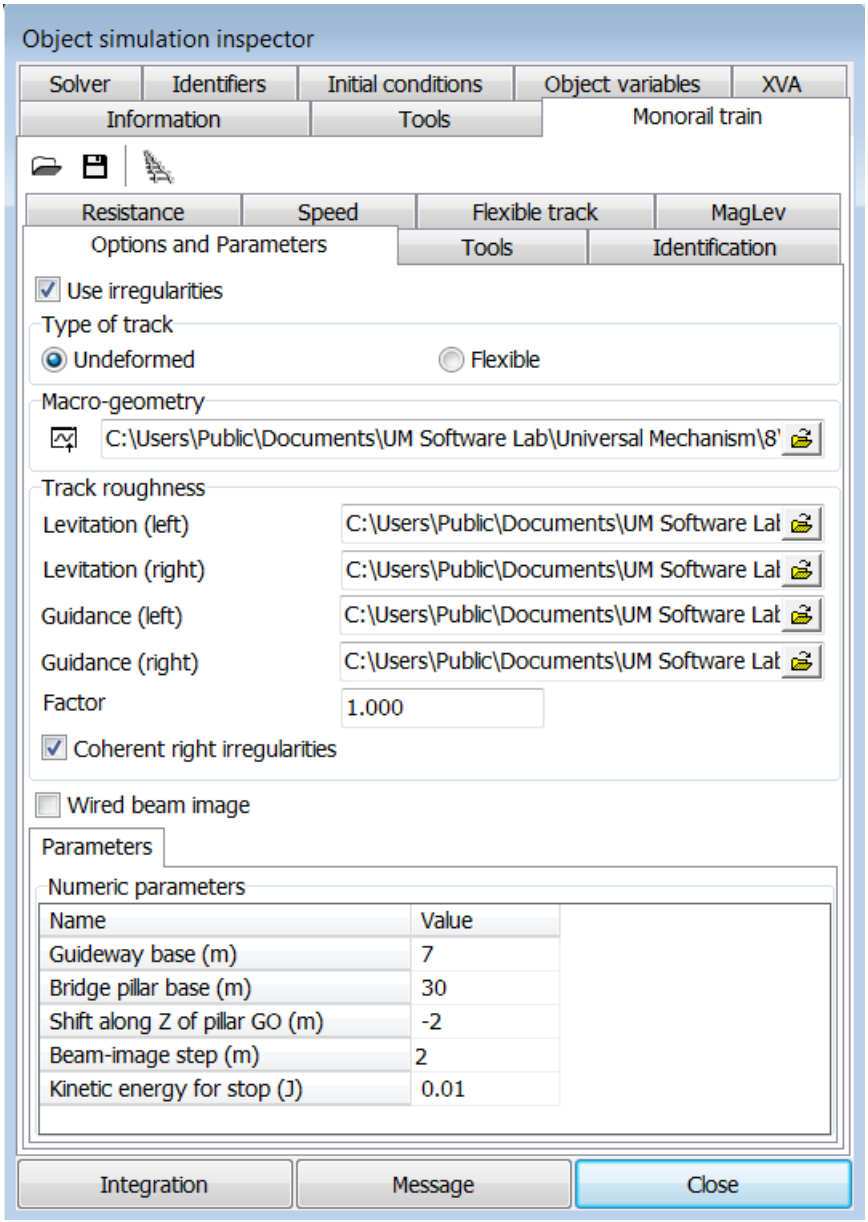

Figure 1.43. Object simulation inspector

The most part of the maglev specific data is entered and modified with the help of the **Monorail train** tab in the **Object simulation inspector**, Figure 1.43. Use the **Analysis | Simulation…** menu command of the **UM Simulation** program to open the inspector.

Here we consider maglev specific parameters.

The maglev simulation parameters are saved in vehicle configuration files *.mrt. Use the buttons on the tab to read/write data.

General information about **UM Simulation** program and its tools are concentrated in Chapter 4.

The user should follow some definite steps to make a new created monorail model ready for simulation.

1. Create a maglev train model in **UM Input** program.
2. Run the **UM Simulation** program.
3. Assign a preliminary created file of macro-geometry by the , Figure 1.43. Use the button to view/modify the macro-geometry.
4. Set levitation and guidance magnet models and parameters.
5. If necessary, set lateral shift of U-shaped levitation magnets to model staggered configuration of magnets, Section 1.8.3 *Staggered configuration of U-core levitation magnets*.
6. Set beam section profile.
7. If necessary, check the option **Use Irregularities** and assign irregularity files, Figure 1.43. The **Factor** increases (<1) or decreases (>1) assigned irregularities.
8. Set the guideway structure geometrical parameters, Figure 1.43:
    - **Guideway base (m)** – distance between two parallel guiding beams, has a visual effect only.
    - **Bridge pillar base (m)** – distance between bridge pillars in longitudinal direction, has a visual effect only.
    - **Shift along Z of pillar go (m)** allows matching the pillar vertical position.
    - **Beam image step (m)** is the discretization step of the longitudinal beam image. Decrease of this parameter makes smother the beam curve in animation window, has a visual effect only.
9. Set the **Kinetic energy for stop** parameter (Figure 1.43), which is used in equilibrium simulation (speed mode v=0).

1.8.2. Maglev control parameters

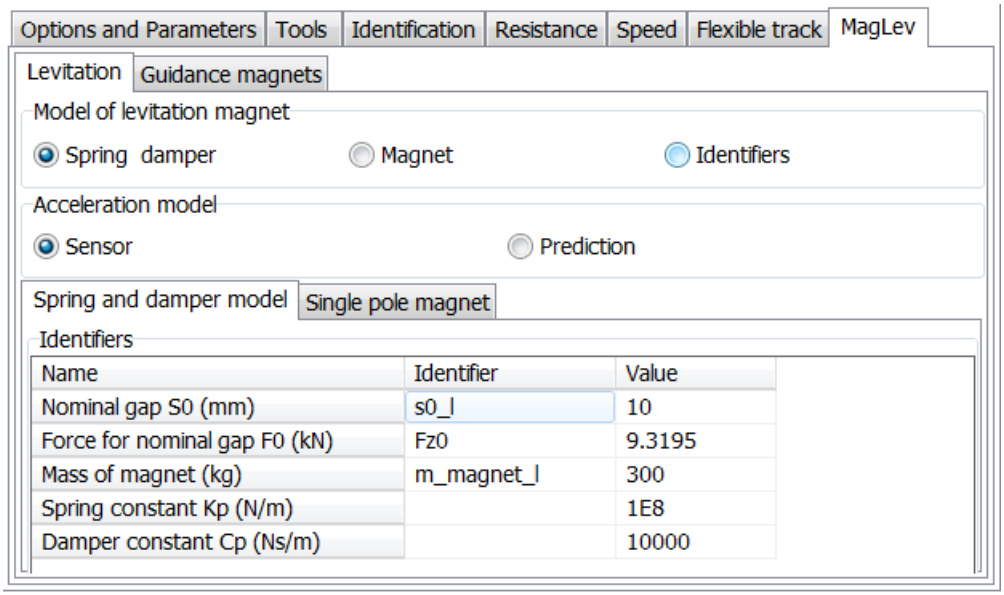

Figure 1.44. Levitation and guidance magnet parameters

The **MagLev** tab in simulation inspector is used for specification of the magnet control parameters, Figure 1.44. Identical sets of parameters are available for levitation and guidance magnets.

Model of levitation magnet

The type of magnet model is selected according to Section 1.6, *Magnet models*.

Acceleration model

If magnet acceleration is used for levitation or/and guidance control (see Section 1.6.2), here the type of acceleration evaluation is selected.

- **Sensor**: acceleration is estimated according to the mechanical sensor data; see Section 1.3.3 *Model of accelerometer*.
- **Prediction**: acceleration is predicted by Lagrangean polynomial of degree 3.

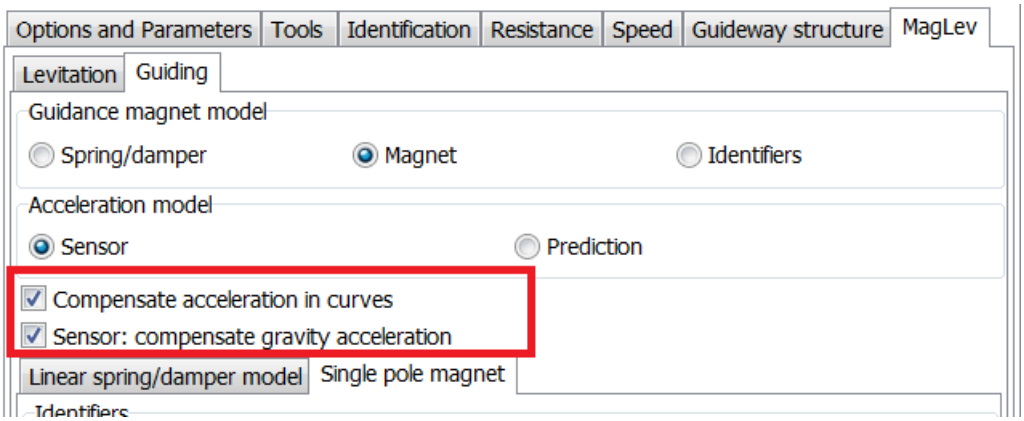

Figure 1.45. Compensation of lateral acceleration

There are some features in computation of the lateral acceleration for guidance control. First, the curving acceleration can be compensated, i.e. the term v^2/R is added to the lateral accelera-

tion or subtracted from it depending on the curve direction right/left. Second, the gravity acceleration due to the rotation of the sensor about the longitudinal axis is compensated from the sensor, i.e. the term αg is subtracted from the accelerometer data, where g is the gravity acceleration, and α is the angle of sensor rotation about the longitudinal axis. The corresponding options are (Figure 1.45):

- **Compensate acceleration in curves**
- **Sensor: compensate gravity acceleration**

An example of compensation for the lateral sensor is shown in Figure 1.46. The left plot compares acceleration without compensation of the acceleration in a curve and two plots with compensation. Compensated accelerations are small and compared in the right figure. The right figure shows that the sensor data for acceleration with compensated gravity is near to zero in the circular curve.

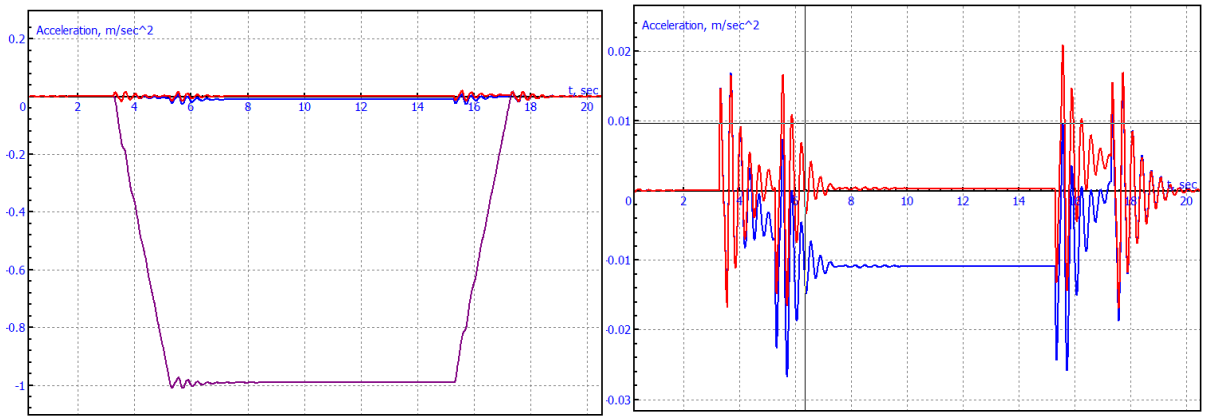

Figure 1.46. Lateral sensor acceleration with and without compensation

Spring and damper model

A table in Figure 1.44 is used for setting parameters of the spring–damper magnet model from Section 1.6.1 *Spring-damper model*.

Remark. It is important that identifiers can be assigned to magnet model parameters. For example, three identifiers from the model list are assigned for the spring and damper magnet control in Figure 1.44, the identifier *s0_l* and so on. To assign an identifier, double click by the left mouse button on the corresponding cell of the table and select the desired identifier, Figure 1.47. These assignments are useful in linear analysis of magnet controls and in multivariant computations.

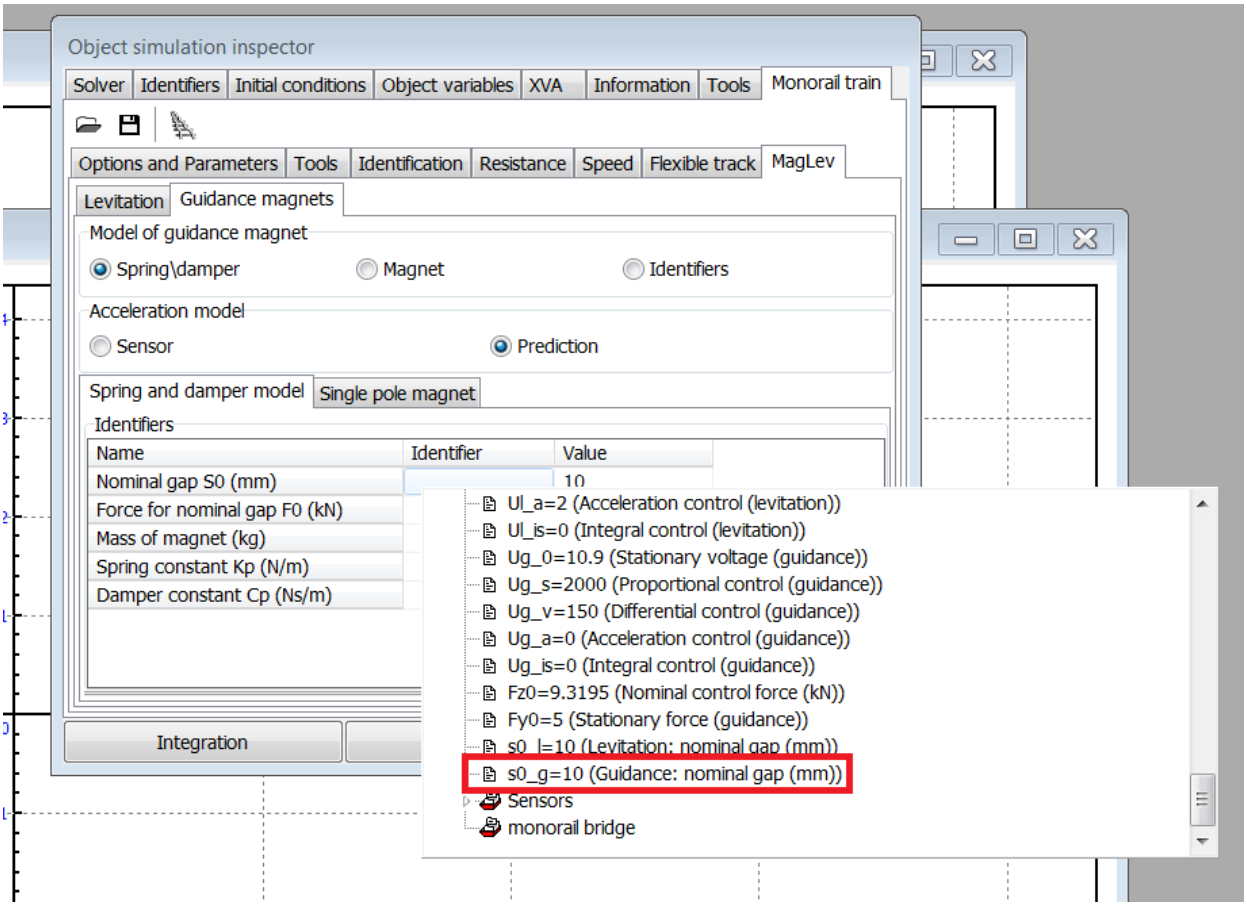

Figure 1.47. Assignment of identifier to the guidance nominal gap

Single pole magnet

The single pole model of magnet is described in Section 1.6.2 *Single pole magnet model*. Both for the levitation and guidance magnet models, the tab contains two groups of parameters: *specified parameters*, which values should be set by the user, and *estimated parameters* automatically computed be the program, Figure 1.48.

Sense of specified parameters is clear from the comments in the table in Figure 1.48. The estimated parameters are computed according to the following formulas from Sections 1.6.2, 1.6.5:

$$I_0 = S_0\sqrt{F_0/\kappa},\ U_0 = RI_0,\ L_0 = \frac{2\kappa}{S_0},\ T = \sqrt{\frac{mS_0}{2F_0}},\ T_i = \frac{L_0}{R},$$

$$U_s^* = \frac{U_0}{S_0}, U_v^* = \frac{U_0 T k_v^*}{S_0}, U_a^* = \frac{U_0 T^2}{S_0},$$

$$k_s = \frac{U_s S_0}{U_0},\ k_v = \frac{U_v S_0}{U_0 T},\ k_a = \frac{U_a S_0}{U_0 T^2},$$

$$k_v^* = \frac{T_i(k_s - 1)}{T(1 + k_a)}.$$

These values help the user to set the correct values of control parameters.

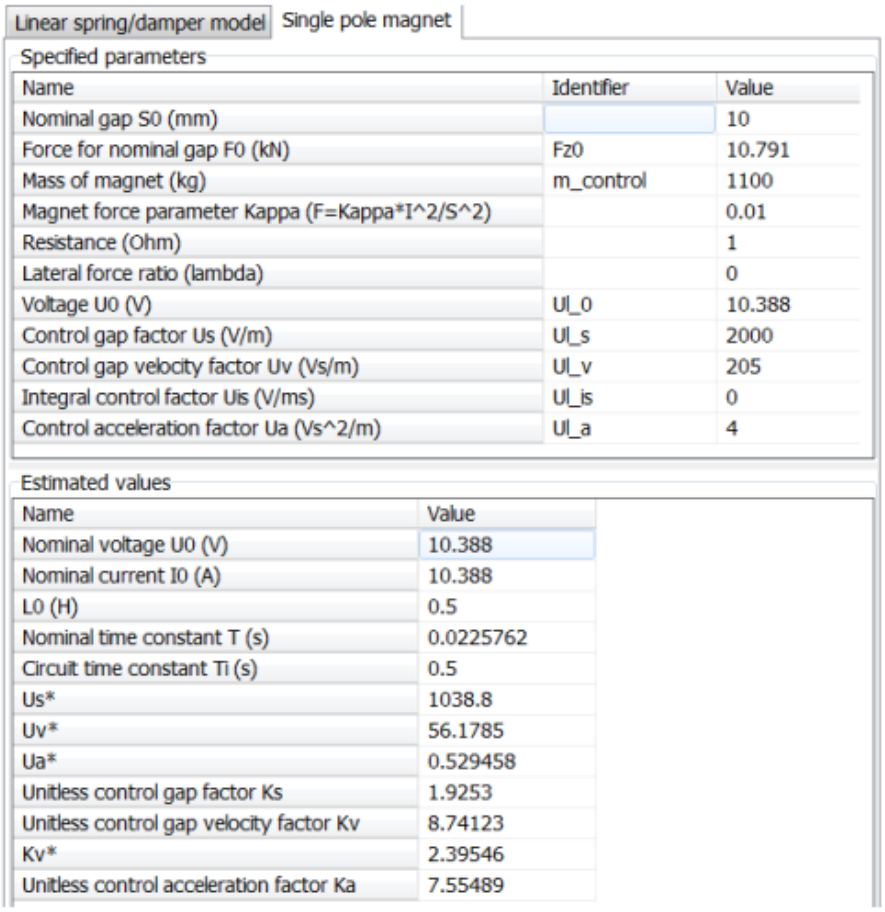

Figure 1.48. Parameters of single pole magnet and control

Remark. The parameter **Lateral force ratio (lambda)** has a positive value for U-shaped magnets. It allows simulating a passive guidance by levitation magnets, Section 1.6.3U-shaped magnet

1.8.3. Staggered configuration of U-core levitation magnets

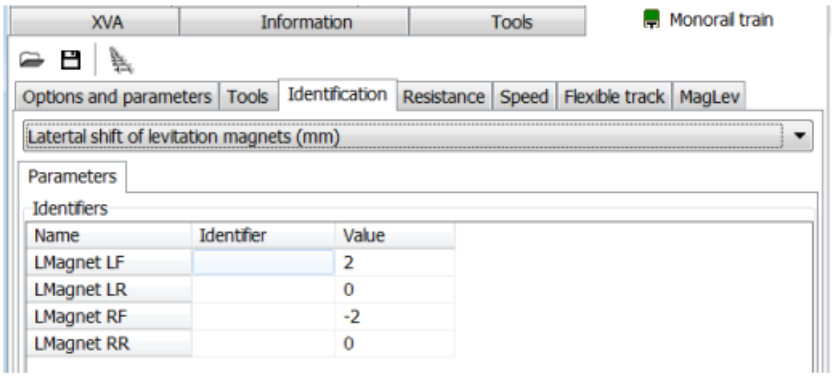

Figure 1.49. Lateral shift of levitation magnets

To model staggered U-shaped levitation magnets [16], set the lateral shift of magnets on the **Monorail train | Identification** tab. Select the **Lateral shift of levitation magnets** item in the drop down menu, Figure 1.49. Shift values are set in millimeters. The positive value corresponds to the shift in the positive Y direction, Figure 1.2. *Base system of coordinates (SC0).*

1.8.4. Additional coordinates for magnet models

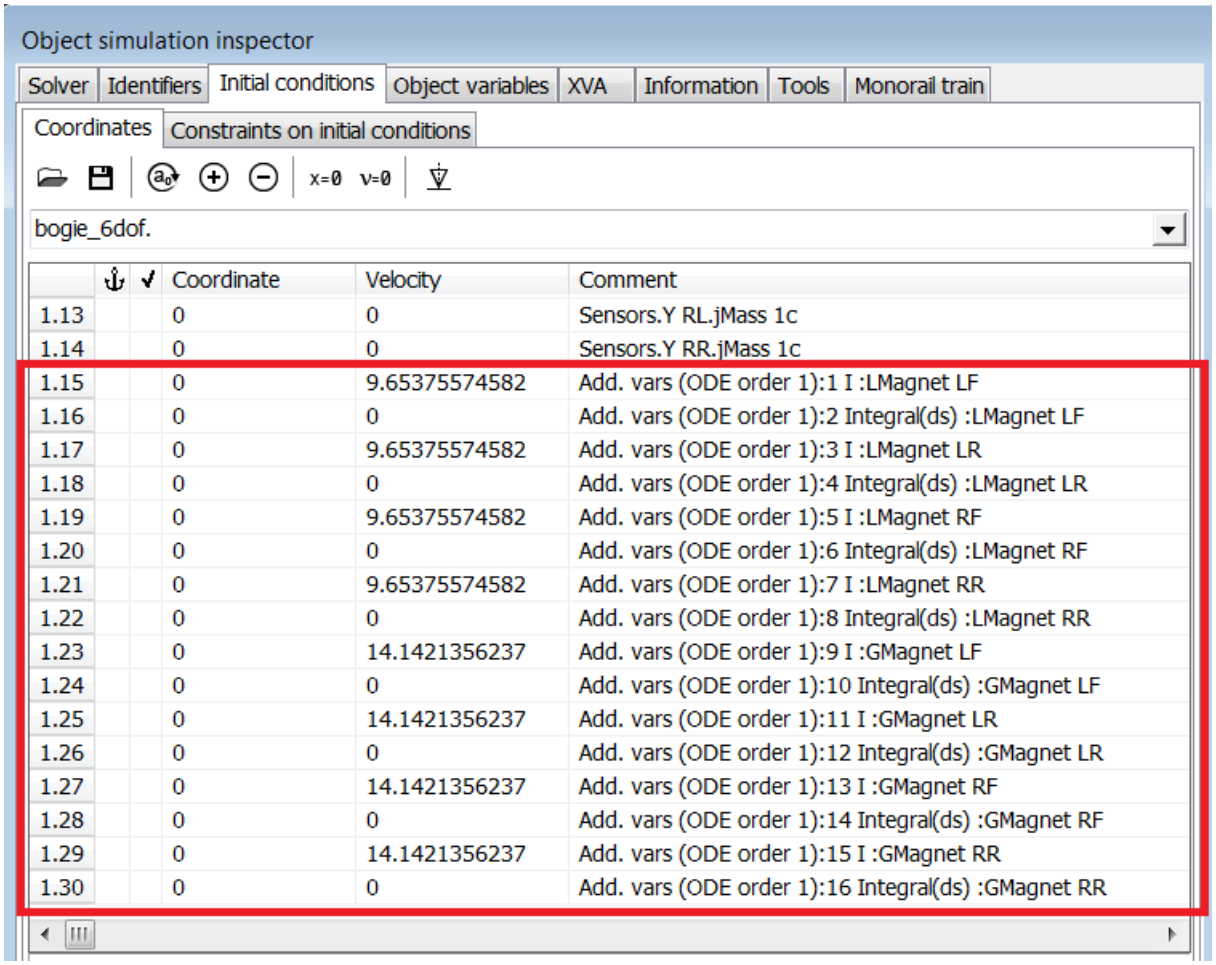

			Coordinate	Velocity	Comment
1.13			0	0	Sensors.Y RL.jMass 1c
1.14			0	0	Sensors.Y RR.jMass 1c
1.15			0	9.65375574582	Add. vars (ODE order 1):1 I :LMagnet LF
1.16			0	0	Add. vars (ODE order 1):2 Integral(ds) :LMagnet LF
1.17			0	9.65375574582	Add. vars (ODE order 1):3 I :LMagnet LR
1.18			0	0	Add. vars (ODE order 1):4 Integral(ds) :LMagnet LR
1.19			0	9.65375574582	Add. vars (ODE order 1):5 I :LMagnet RF
1.20			0	0	Add. vars (ODE order 1):6 Integral(ds) :LMagnet RF
1.21			0	9.65375574582	Add. vars (ODE order 1):7 I :LMagnet RR
1.22			0	0	Add. vars (ODE order 1):8 Integral(ds) :LMagnet RR
1.23			0	14.1421356237	Add. vars (ODE order 1):9 I :GMagnet LF
1.24			0	0	Add. vars (ODE order 1):10 Integral(ds) :GMagnet LF
1.25			0	14.1421356237	Add. vars (ODE order 1):11 I :GMagnet LR
1.26			0	0	Add. vars (ODE order 1):12 Integral(ds) :GMagnet LR
1.27			0	14.1421356237	Add. vars (ODE order 1):13 I :GMagnet RF
1.28			0	0	Add. vars (ODE order 1):14 Integral(ds) :GMagnet RF
1.29			0	14.1421356237	Add. vars (ODE order 1):15 I :GMagnet RR
1.30			0	0	Add. vars (ODE order 1):16 Integral(ds) :GMagnet RR

Figure 1.50. Additional magnet variables

Two additional coordinates are used for each of the magnet, if the *Single pole magnet model* is selected (Figure 1.50):

Current in magnet circuit I, Section 1.6.2

Integral of the gap deviation on the nominal value $I_S = \int_0^t \Delta S dt$

Both of the coordinates satisfy first order ODEs

$$\frac{d(LI)}{dt} = -RI + U,$$

$$\frac{dI_S}{dt} = \Delta S.$$

UM solves second order ODEs, that is why the first order are converted to the second order as

$$\frac{dq}{dt} = I, \quad \frac{d(LI)}{dt} = -RI + U,$$

$$\frac{dQ_S}{dt} = I_S, \quad \frac{dI_S}{dt} = \Delta S.$$

Thus, the q, Q_s variables are computed, and I, I_s are their time derivatives. Please note that the initial values for the circuit current in Figure 1.50 are set to the time derivative of coordinates in the **Velocity** column.

If not the simple pole magnet model is used for computation of magnet forces, the additional variables are ignored.

1.8.5. Speed control

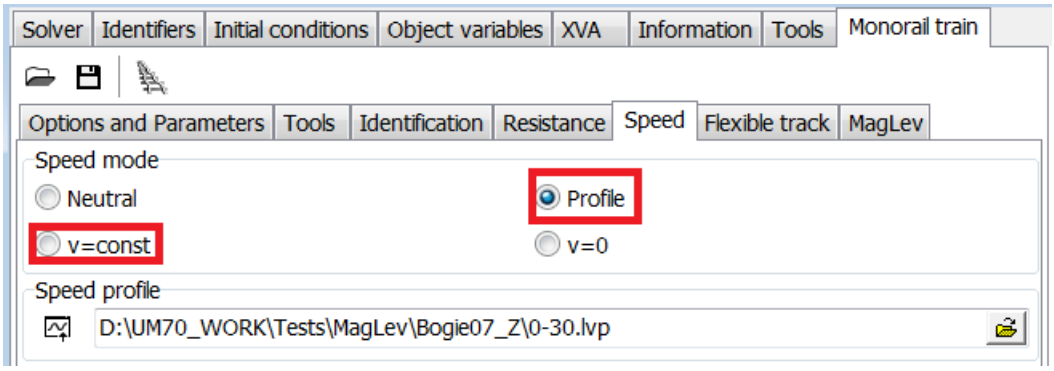

Figure 1.51. Vehicle speed options

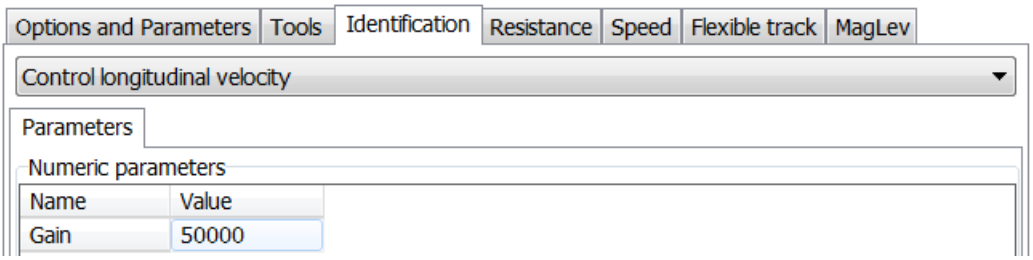

Figure 1.52. Speed control gain

If constant speed or a profiles speed modes are selected (Figure 1.51), the speed control force if applied to the magnets in the longitudinal direction. The control force is computed as

$$F = -\frac{K(v - v_d)}{N_m},$$

where K is the control gain (Figure 1.52), v is the current velocity of the vehicle, v_d is the desired velocity, and N_m is the number of magnets.

An example of speed profile as well as simulation speed is shown in Figure 1.53.

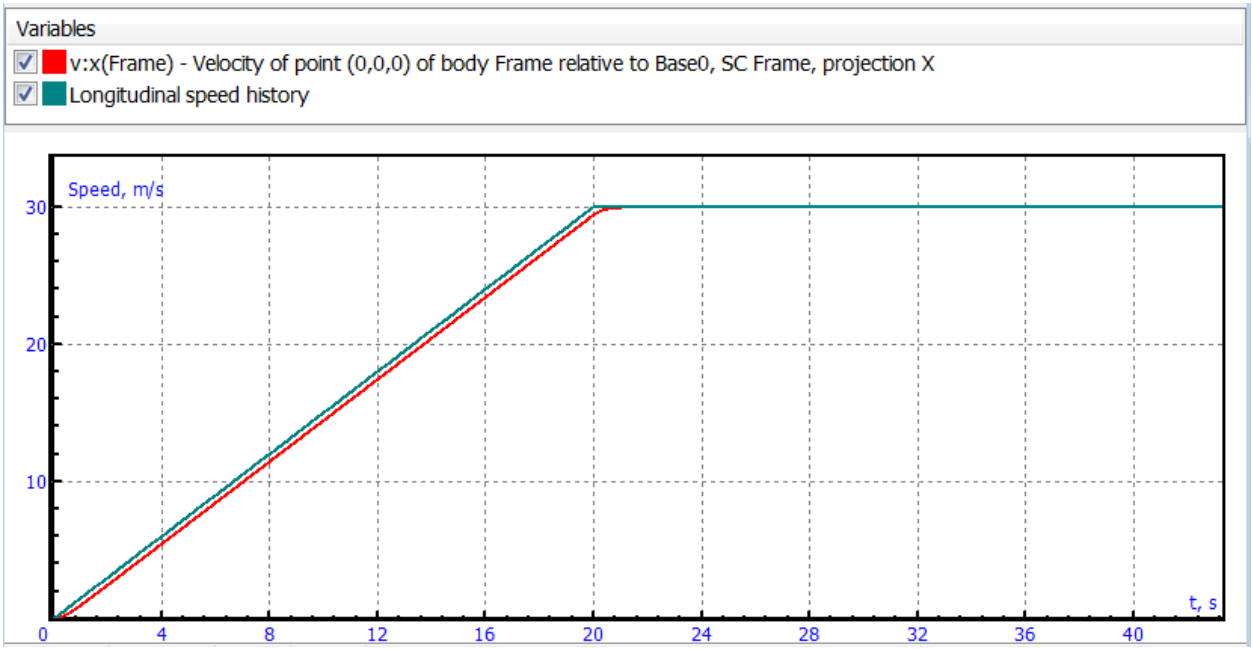

Figure 1.53. Comparison of desired and simulation speed

1.8.6. Maglev train specific variables

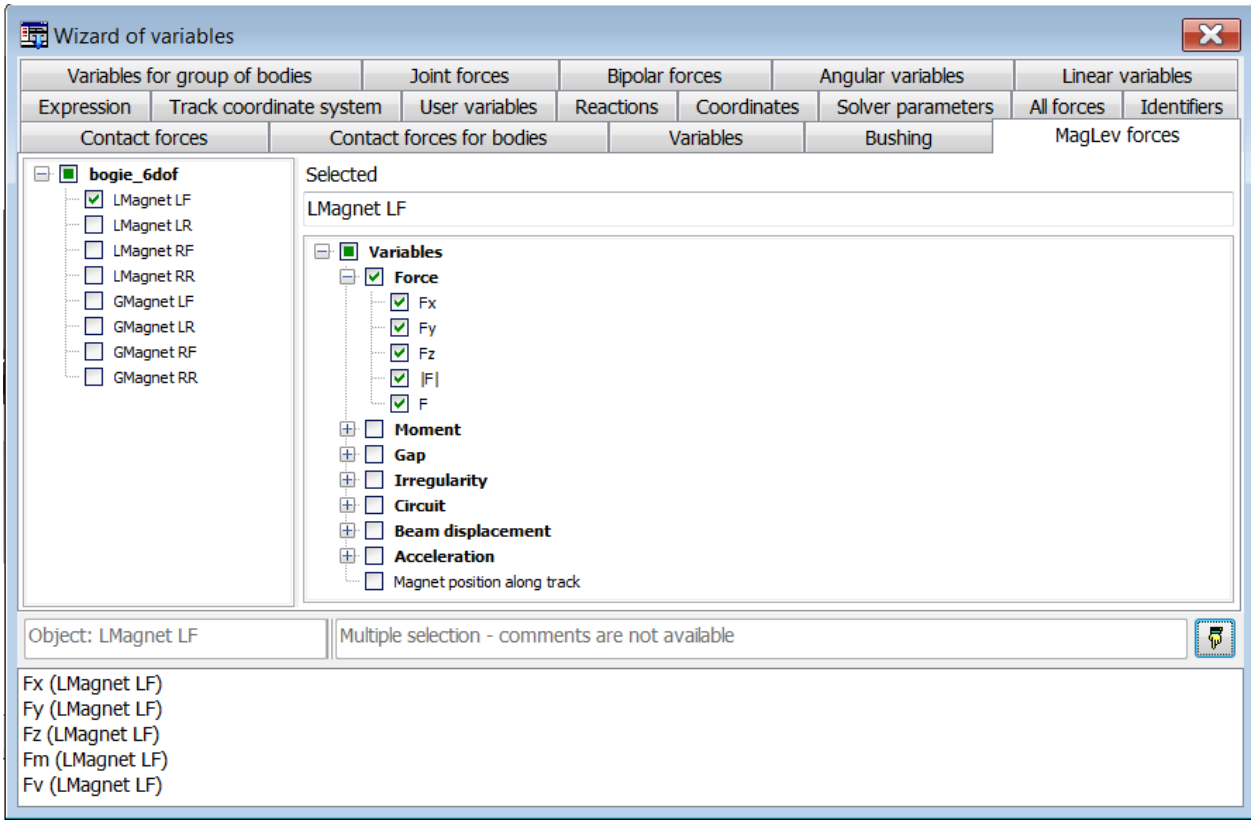

Figure 1.54. Maglev forces

Magnet variables are available on the **MagLev forces** tab of the **Wizard of variables**, Figure 1.54. Use the **Tools | Wizard of variables…** menu command to open this window.

Use other tabs of the wizard to create kinematic and dynamic variables different from the magnet variables.

See Chapter 4 to get information about creating variables and their usage.

1.8.6.1. Force, Moment

The variable corresponds to magnet forces (Figure 1.54) and moments:

- Fx(Mx) – projection on longitudinal direction of the track system of coordinates;
- Fy(My) – projection on lateral direction of the track system of coordinates;
- Fz(Mz) – projection on vertical direction of the track system of coordinates (upwards positive);
- |F|(|M|) – module of force/moment;
- F(M) – vector of force/moment.

Force and moment variables are measured in kN, kN·m.

If a spring-damper or a single magnet models are used for computation of magnet forces, the moment value is zero, and Fz or Fy force components are available only for the levitation or guidance magnets respectively, Sections 1.6.1, 1.6.2.

External magnet models are applied by the user, non-zero components depend on the model, and the forces components are available through the corresponding identifiers as well.

1.8.6.2. Gap

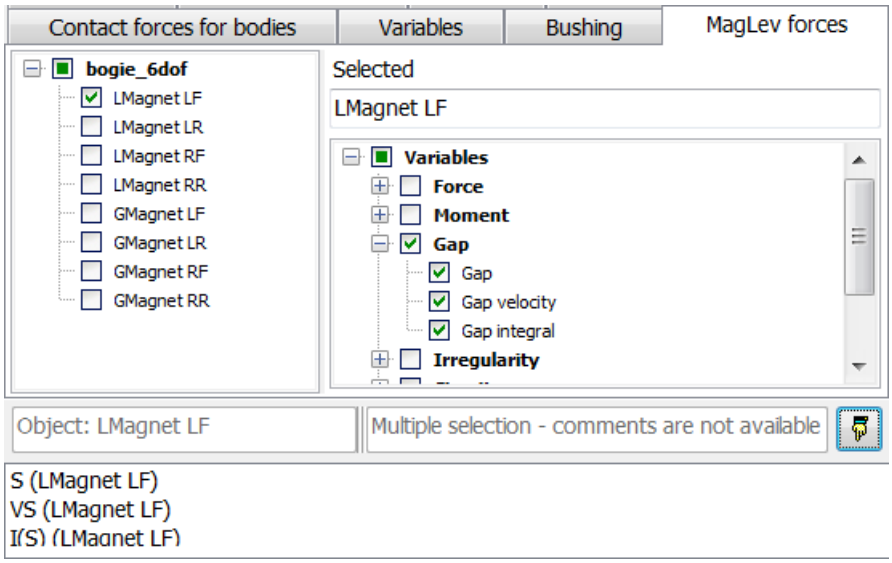

Figure 1.55. Magnet gap

The gap variables

$$S,\ \dot{S},\ \int_0^t \Delta S dt$$

are available for all magnet models, see Section 1.6.2 *Single pole magnet model*.

The gap is measured in mm and takes into account the track irregularities.

1.8.6.3. Lateral shift

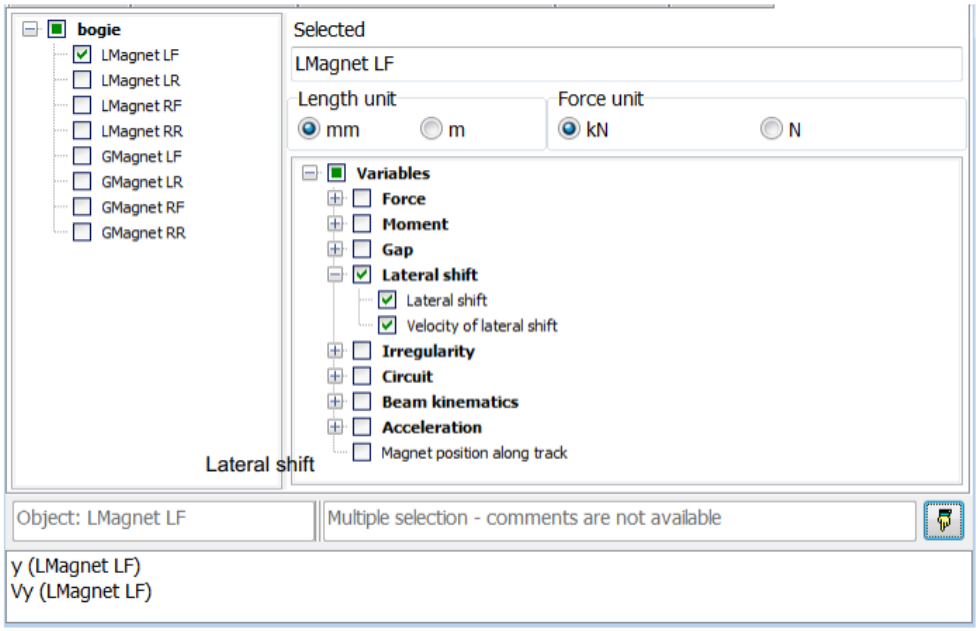

Figure 1.56. Lateral shift of magnets

The variables compute the lateral shift y of magnets and its time derivative $\dot{y}$. The magnet shift is used for computation of lateral force in the case of U-shaped electromagnets, Section 1.6.3 *U-shaped magnet*.

1.8.6.4. Irregularity

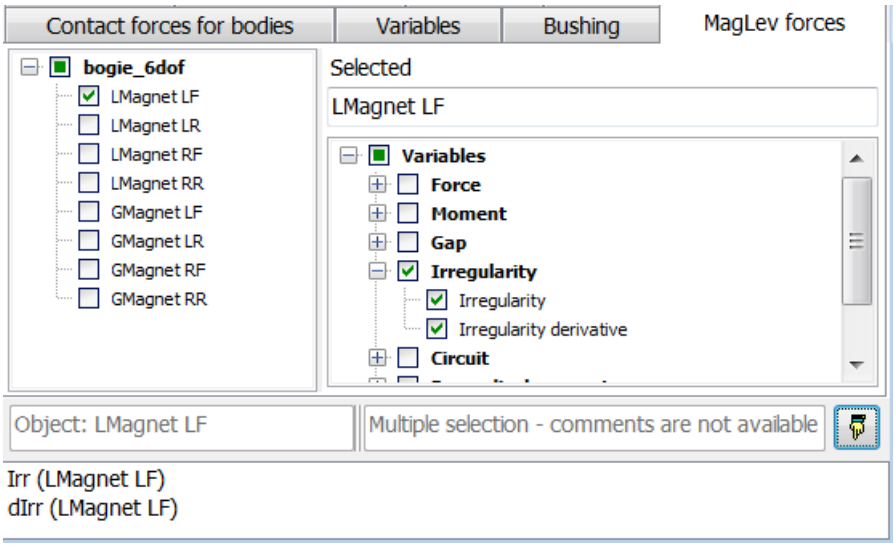

Figure 1.57. Irregularity variable

The variables correspond to the track roughness for levitation and guidance magnets as well as their derivatives with respect to the distance. The irregularity is measured in mm, its derivative is unitless.

1.8.6.5. Circuit

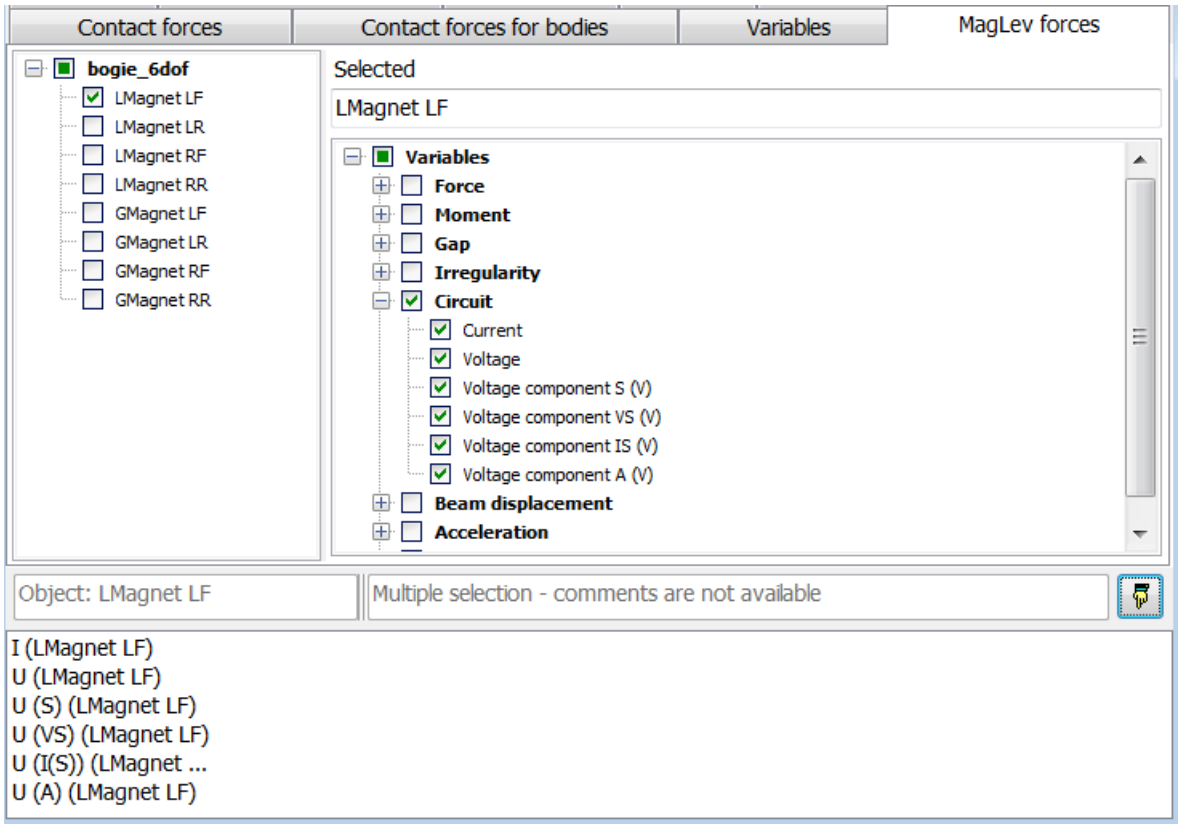

Figure 1.58. Magnet circuit variables

The variable corresponds to the circuit variables according to the *Single pole magnet model*:

- I – Current (A),
- U – voltage (V),
- $U_s \Delta S$ – voltage component S (V),
- $U_v \dot{S}$ – voltage component S (V),
- $U_{is} \int_0^t \Delta S dt$ – voltage component IS (V),
- $-U_a \ddot{Z}$ – voltage component A (V).

1.8.6.6. Beam displacements

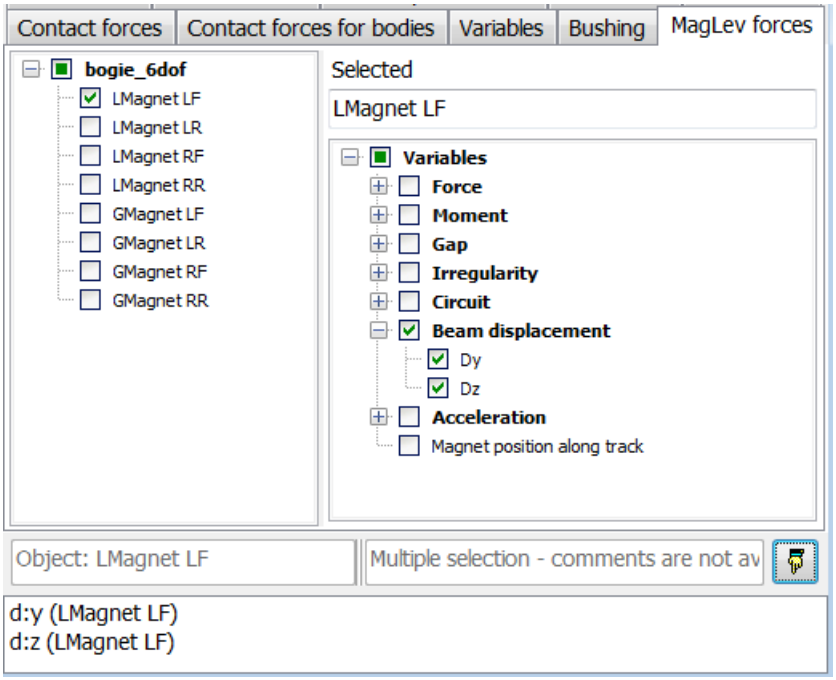

Figure 1.59. Flexible beam deflections

These variables are used if the flexible beam track model is used. The variables correspond to the lateral and vertical beam deflections in the magnet force position.

The deflections are measured in mm.

1.8.6.7. Acceleration

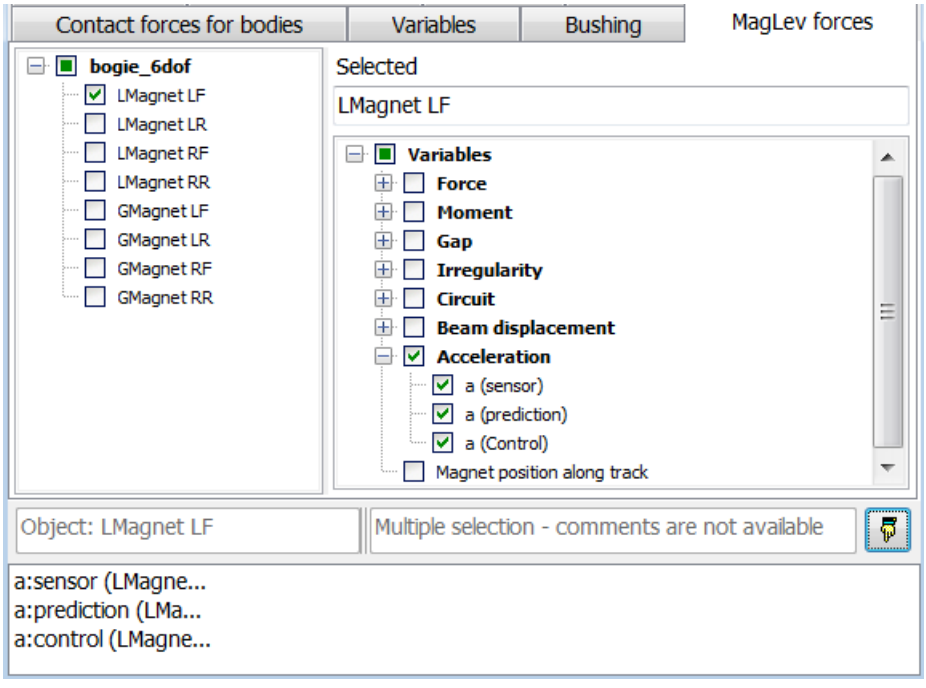

The variables correspond to vertical accelerations of levitation magnets and lateral acceleration of guidance magnet relative to then track system of coordinates. Accelerations are measured

in m/s^2. The '*Control*' corresponds to compensated acceleration, if the compensation option is checked, Section 1.8.1 *Preparing for simulation*.

1.8.6.8. Magnet position along the track

The variable corresponds to the position of the magnet along the track and computed according to the formula

$$L = l_0 + l(t)$$

where l_0 is the initial position of the magnet point is SC0 (the base coordinate system, Section 1.2), and $l(t)$ is the distance along the track from the motion start.

1.8.7. Kinematic characteristics relative to track system of coordinates

Kinematical variables of bodies should be often projected on the track system of coordinates (TSC). The X-axis of the TSC is the tangent to the guiding beam centerline including the beam vertical slope; the Y-axis is perpendicular to the X-axis taking into account the superelevation.

Note that axes of the TSC and SC0 in a straight track are parallel, and projections of vectors on these SC are the same.

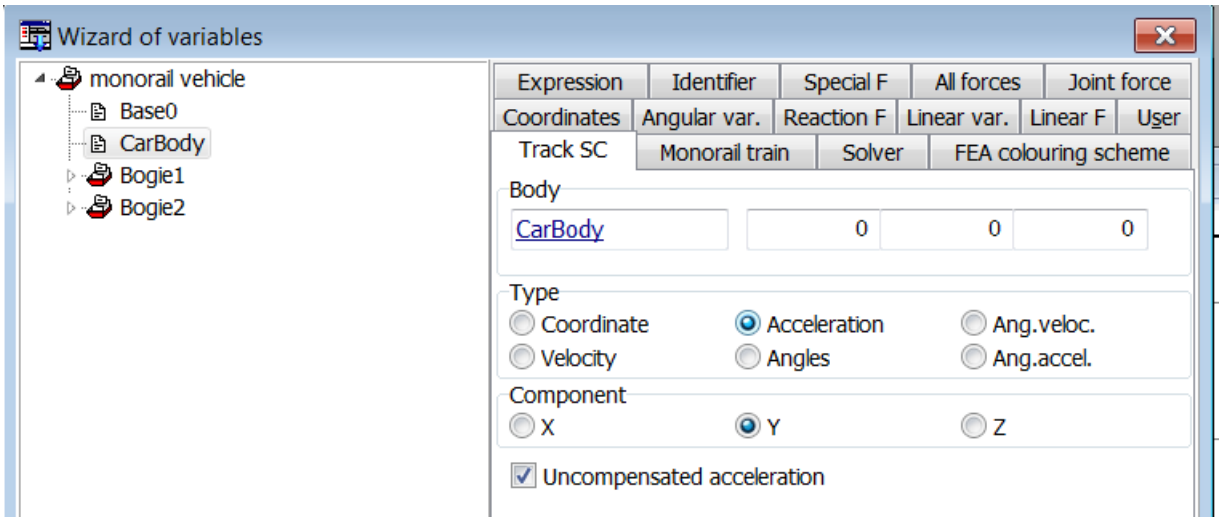

Figure 1.60. Kinematic characteristics of bodies in the track SC

Use the **Track SC** tab of the Wizard of variables to get any kinematic variable in projection of the TSC. To create a variable, perform the following steps:

- select a body in the list in the left part of the wizard;
- select the type of variable: a linear variable (Cartesian coordinates, velocity or acceleration) or an angular variable (angles, angular velocity and angular acceleration);
- set a point in SC of the body, which coordinate, velocity or acceleration should be computed, if a linear variable is selected;
- set an axis of the TSC for projection.

For the lateral component of acceleration, either the uncompensated acceleration or the usual acceleration is selected (Figure 1.60).

1.9. Maglev static and linear analysis

Analysis of linearized equations of maglev vehicles as a very important tool, which allows the user to analyze the stability of levitation and guidance systems, and well as to evaluate proper values of control parameters. Detailed information about this tool can be found in the user's manual file Chapter 4. Here we consider some features of this analysis related to maglev systems.

1.9.1. Computation of equilibrium position

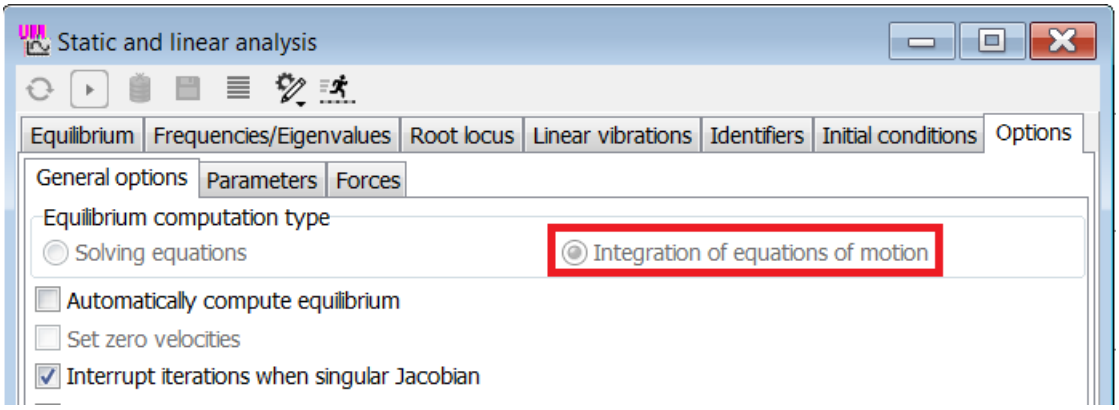

Figure 1.61. SLA options for maglev vehicle

Computation of equilibrium position is possible by the integration method, Figure 1.61. The reason for this limitation is the following: solving nonlinear equilibrium equations by the Newton-Raphson method does not converge for single pole and external magnet models.

It is recommended to compute the equilibrium position by simulation at v=0 speed mode, and uncheck the **Automatically compute equilibrium option**, Figure 1.61.

1.9.2. Frequencies and eigenvalues

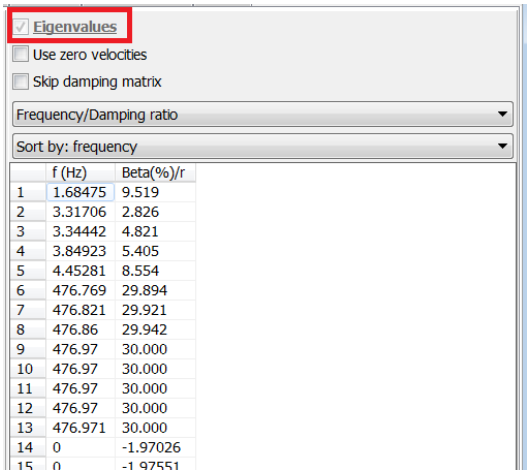

Magnet forces are non–conservative ones, and computation of natural frequencies is correct for the spring–damper magnet models only. Moreover, in the case of external modeling magnet

forces, neither frequencies nor eigenvalues are correct because equations for magnets are not available.

Evaluation of eigenvalues is recommended for the single pole magnet models. If acceleration control is used, the *sensor* type of acceleration computation is necessary; use of *predicted* acceleration leads to wrong results equivalent to $U_a = 0$, see Figure 1.44.

1.9.3. Root locus

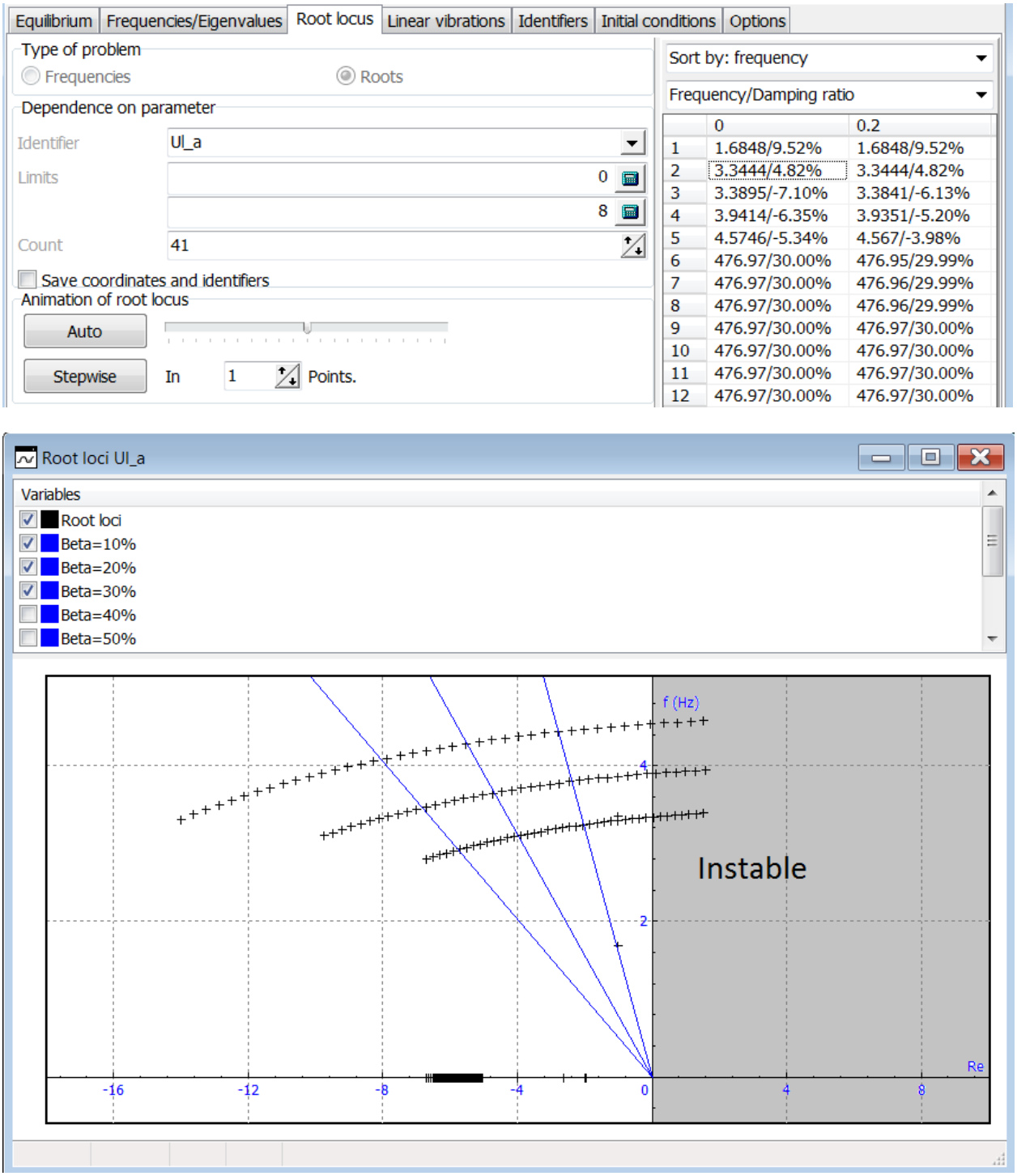

Figure 1.62. Root loci

Root loci give the most useful tool for choice rational values of control parameters in the case of the single pole magnet model. Parameterization of control parameters by identifiers allows computing eigenvalues loci and drawing conclusions on stability and damping level both the levitation and guidance systems, Section *Identifiers for magnet control*. For example, analysis of stability and damping ratio in dependence on the control parameter U_a parameterized by the identifier *Ul_a* is presented in Figure 1.62.

1.10. Test cases

Here we consider some simulation tests with maglev models.

1.10.1. Equilibrium with disabled magnets

Consider the bogie model {UM Data}\Samples\MagLev\Bogie_6DOF.

1. Load the model.

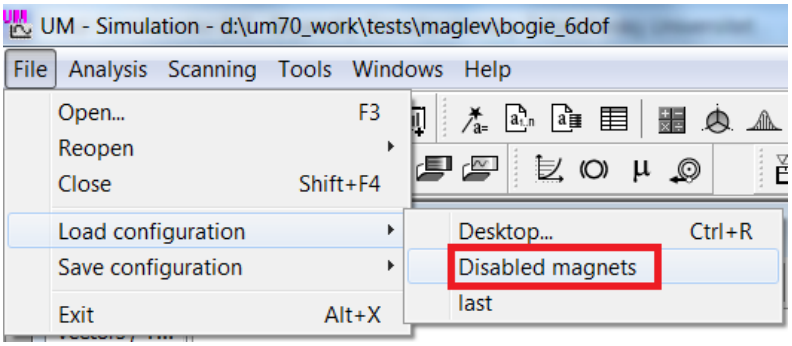

Figure 1.63. Configuration 'Disabled magnets'

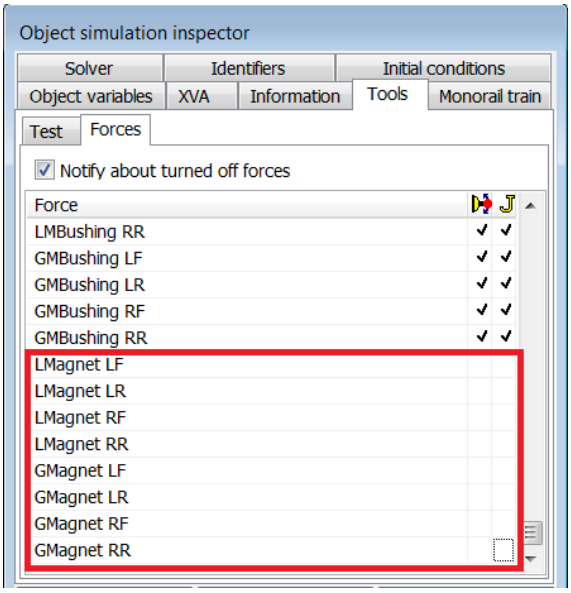

Figure 1.64. Disabled force elements

2. Read the *Disabled magnets* configuration, Figure 1.63. In this configuration we made disabled all the magnets, Figure 1.64. Thus, this test corresponds to the bogie positioning on the upper contacts, Section *Sliding contact elements*.

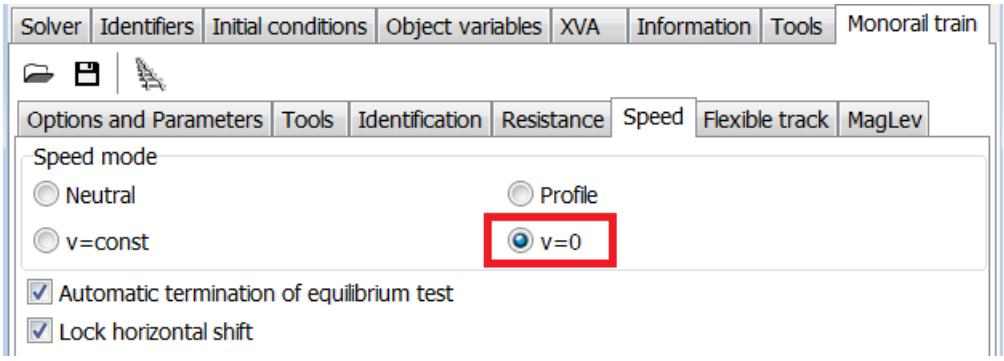

Figure 1.65. Zero speed mode

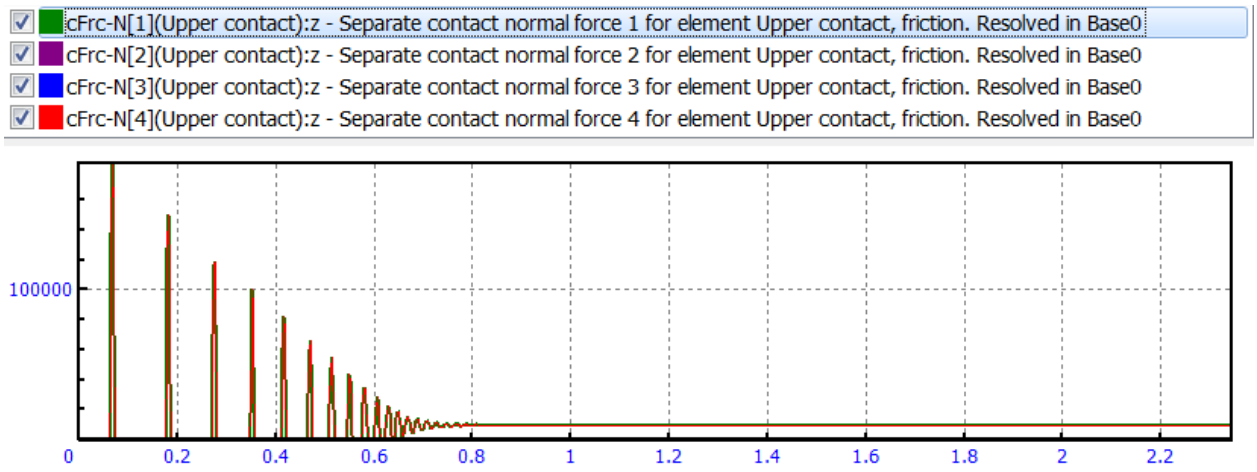

Figure 1.66. Contact forces vs. time

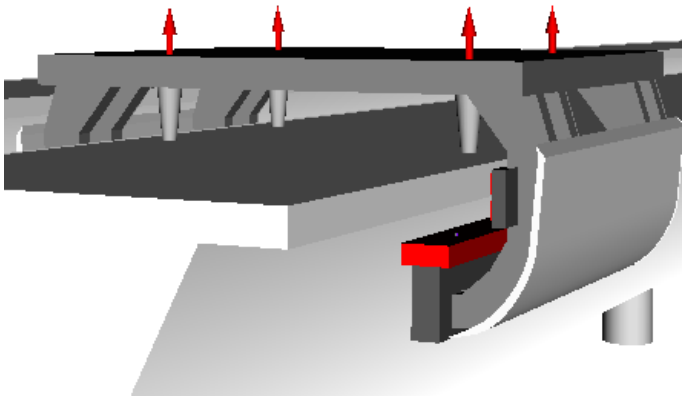

Figure 1.67. Contact forces

3. Run simulation. The speed mode is v=0, Figure 1.65 and simulation stops after the kinetic energy becomes small enough. Initial coordinates are zeroes, and the equilibrium position is achieved after a series of collisions, Figure 1.66. Four read vectors in Figure 1.67 correspond to the normal contact forces.

1.10.2. Bogie uplifting

1. Load the model {UM Data}\Samples\MagLev\Bogie_6DOF.

2. Read the *Uplifting* configuration. In this configuration, all magnets are enabled and the single pole magnet model is used. Initial position of the bogie corresponds to it equilibrium position on contacts according to the test *Equilibrium with disabled magnets*. The value of voltage U0=9.654 V is equal to the nominal value for the nominal gap 10mm. The integral control parameter U_{is} (Section *Single pole magnet model*) is zero.

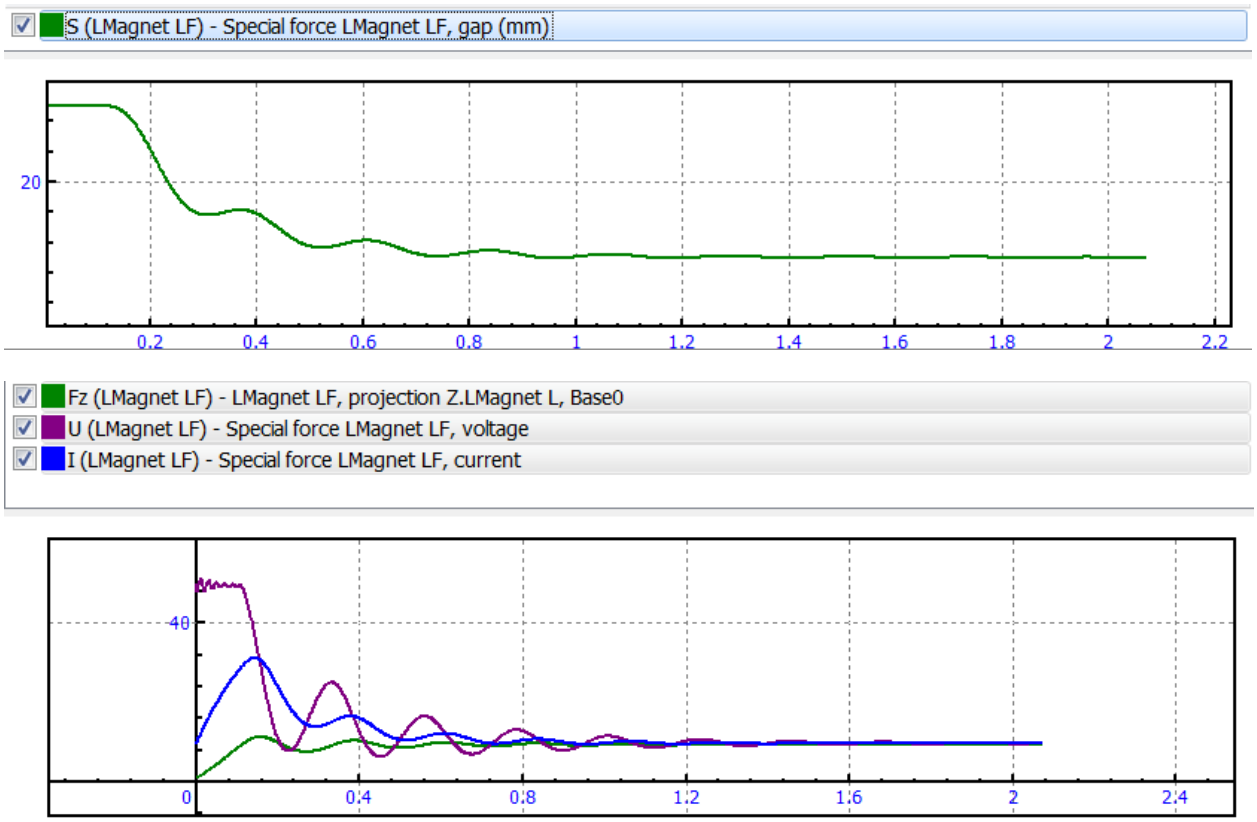

Figure 1.68. Uplifting test variables

3. Run simulation. Some plots for the uplifting process are shown in Figure 1.68.

4. Now consider effects on use of the integral control U_{is} parameter. Reload the *Uplifting* configuration and set zero levitation magnet voltage U0, Figure 1.69.

5. Run simulation for different value of integral control parameter U_{is}, Figure 1.70. It is clear, that there is a static deviation of the gap from the nominal value for zero integral control.

Spring and damper model | Single pole magnet

Specified parameters

Name	Identifier	Value
Nominal gap S0 (mm)		10
Force for nominal gap F0 (kN)	Fz0	9.3195
Mass of magnet (kg)	m_control	950
Magnet force parameter Kappa (F=Kappa*I^2/S^2)		0.01
Resistance (Ohm)		1
Voltage U0 (V)	Ul_0	0
Control gap factor Us (V/m)	Ul_s	2000
Control gap velocity factor Uv (Vs/m)	Ul_v	200
Integral control factor Uis (V/ms)	Ul_is	0
Control acceleration factor Ua (Vs^2/m)	Ul_a	2

Figure 1.69. Levitation magnet control parameters

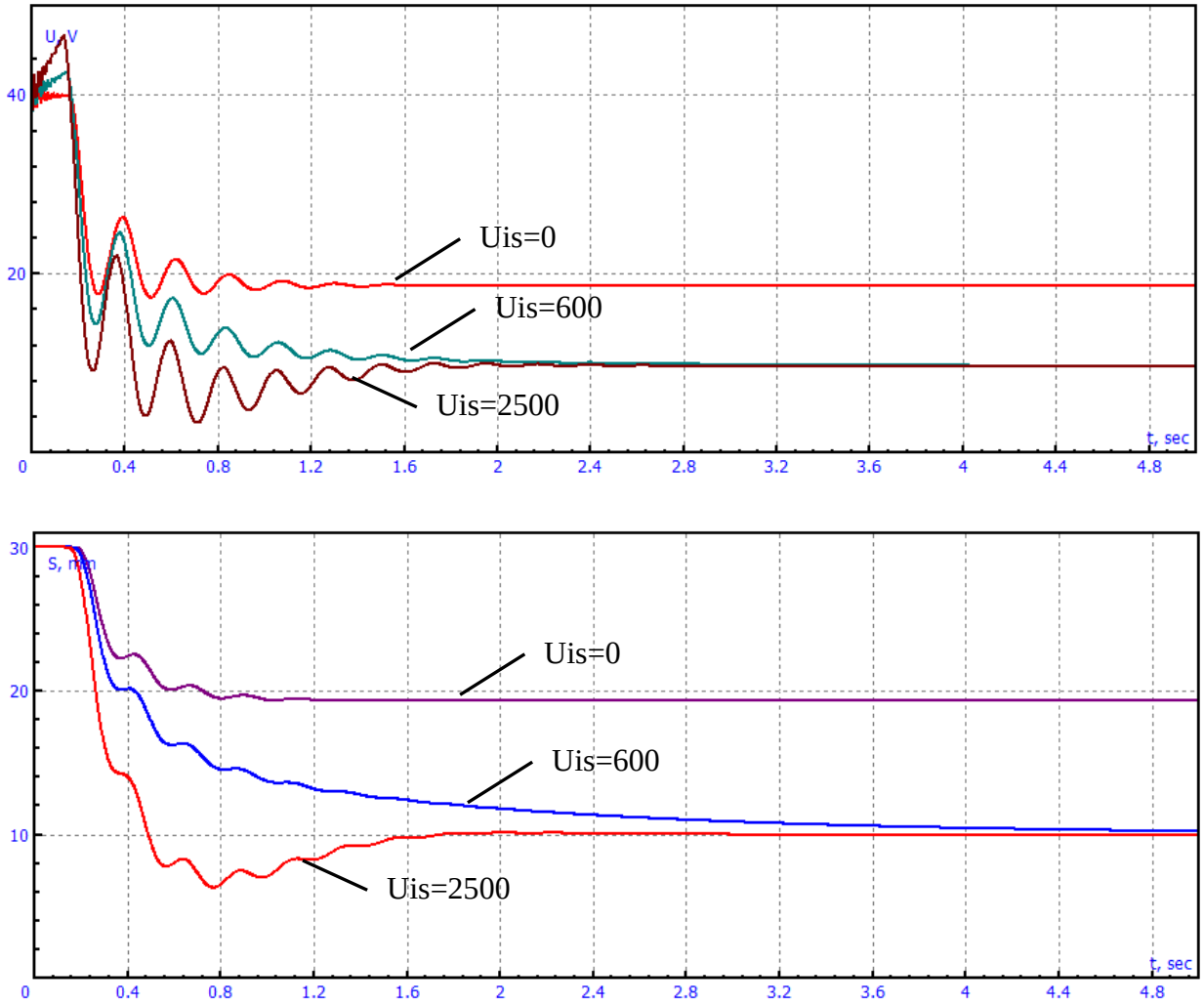

Figure 1.70. Voltage and gap for different integral control

1.10.3. Stability: comparison of simulation with theory

In this section we compare theoretical results on levitation stability with simulation results.

1. Load the model {UM Data}\Samples\MagLev\Bogie_6DOF.
2. Read the *Stability* configuration. The model is in equilibrium position at v=0 speed mode.

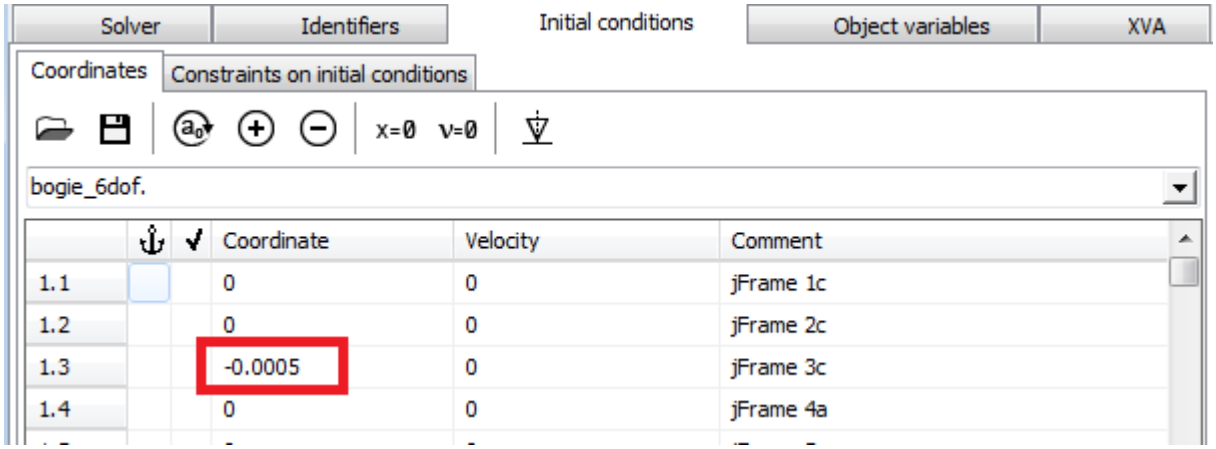

Figure 1.71. Initial deviation of frame from equilibrium

3. Set a deviation of the frame from the equilibrium position 2mm, Figure 1.71.

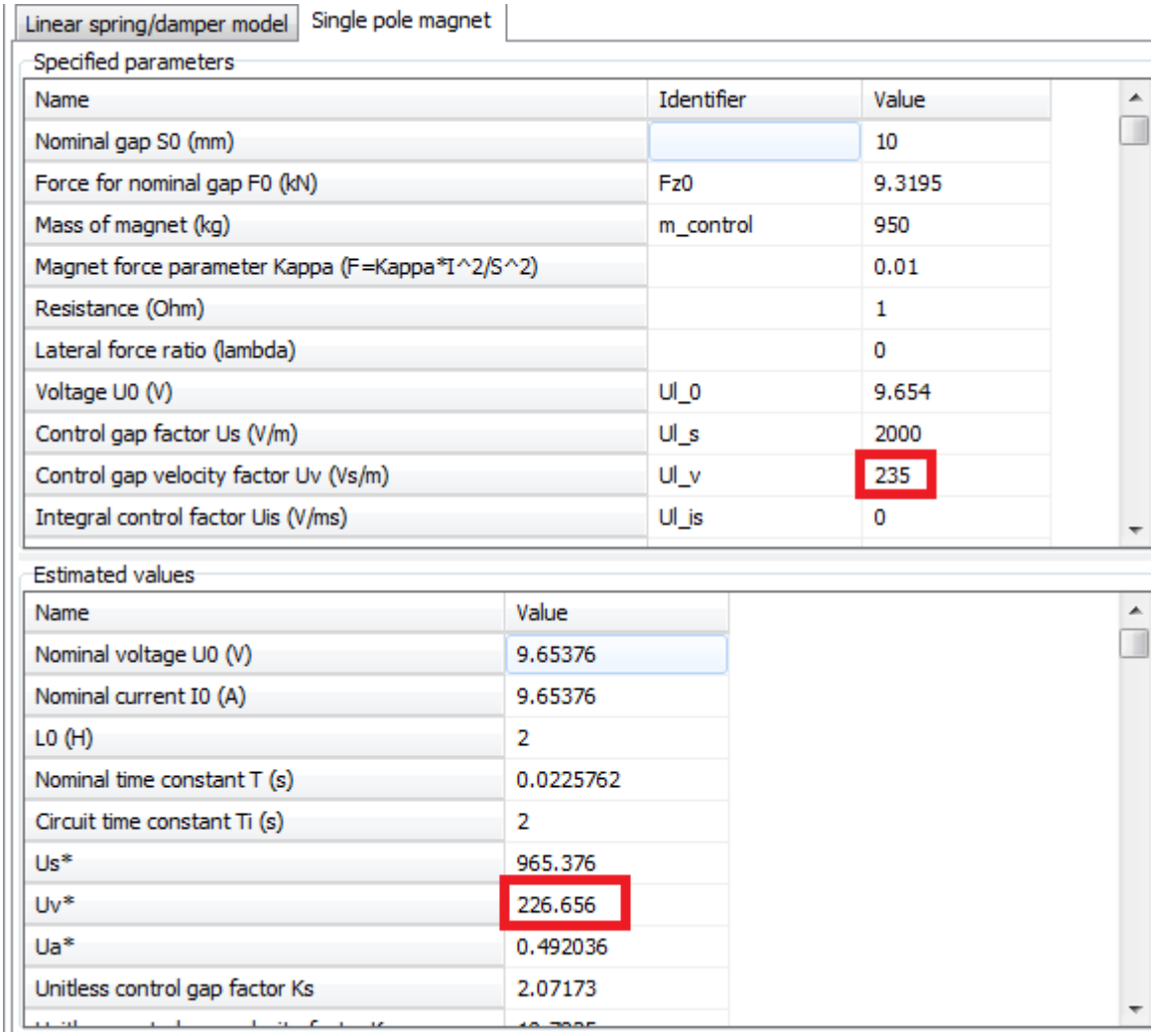

Figure 1.72. Boundary value of control parameter Uv*

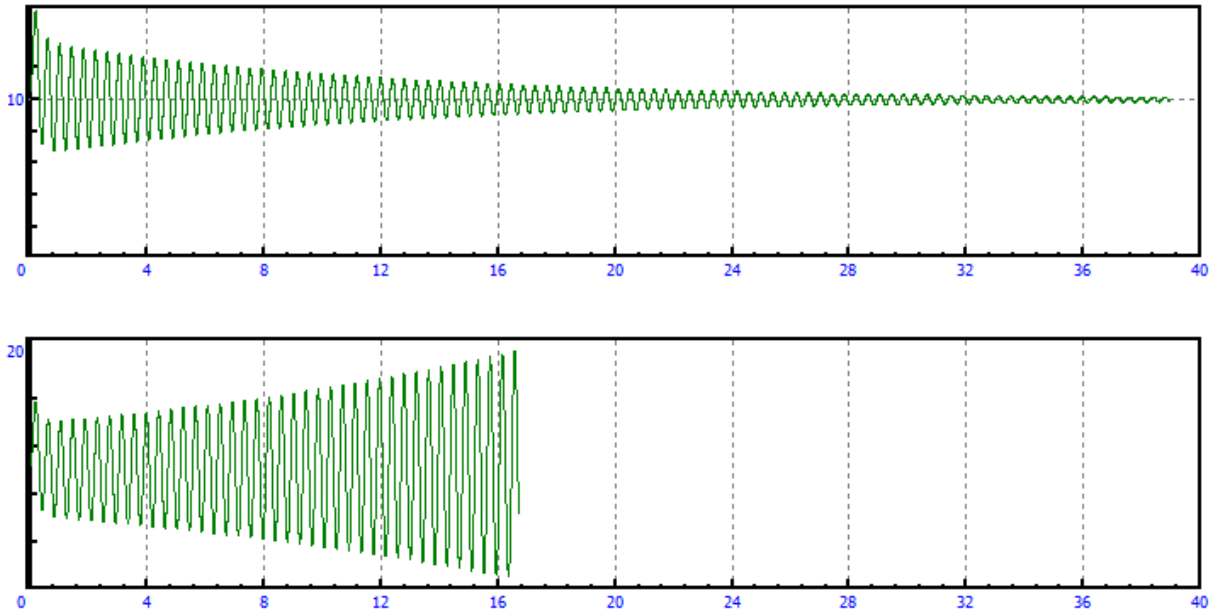

Figure 1.73. Stable and instable levitation

4. Set the control parameter Uv=235 a bit more than the boundary stable value Uv*, Figure 1.72. Run simulation. Now change Uv to 220, which is instable, Figure 1.73.

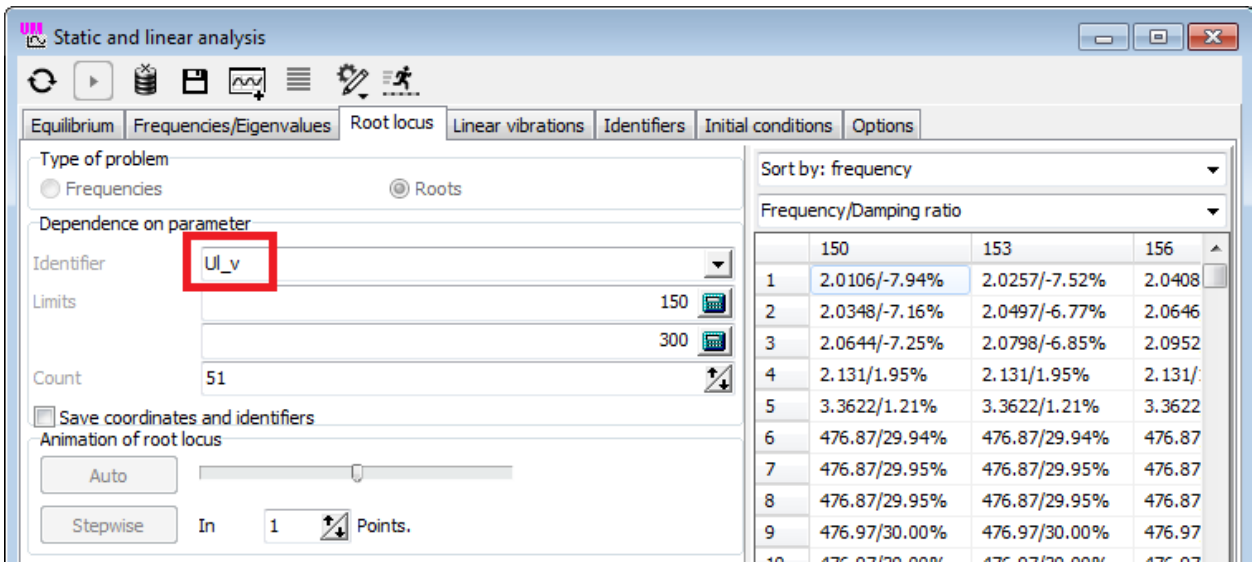

Figure 1.74. Verification of stability by root locus

Let us analyze the stability of levitation with linear analysis.

5. Set the frame vertical coordinate to zero and open the SLA (static and linear analysis) window.

6. Open the **Root locus** tab, select the *Ul_v* identifier and set the interval for analysis like in Figure 1.74. Run root locus computation by the button, and draw roots by the button. Click on the **Stepwise** button to animate the locus. Verify that the stability bound corresponds to the theoretical results, Figure 1.75.

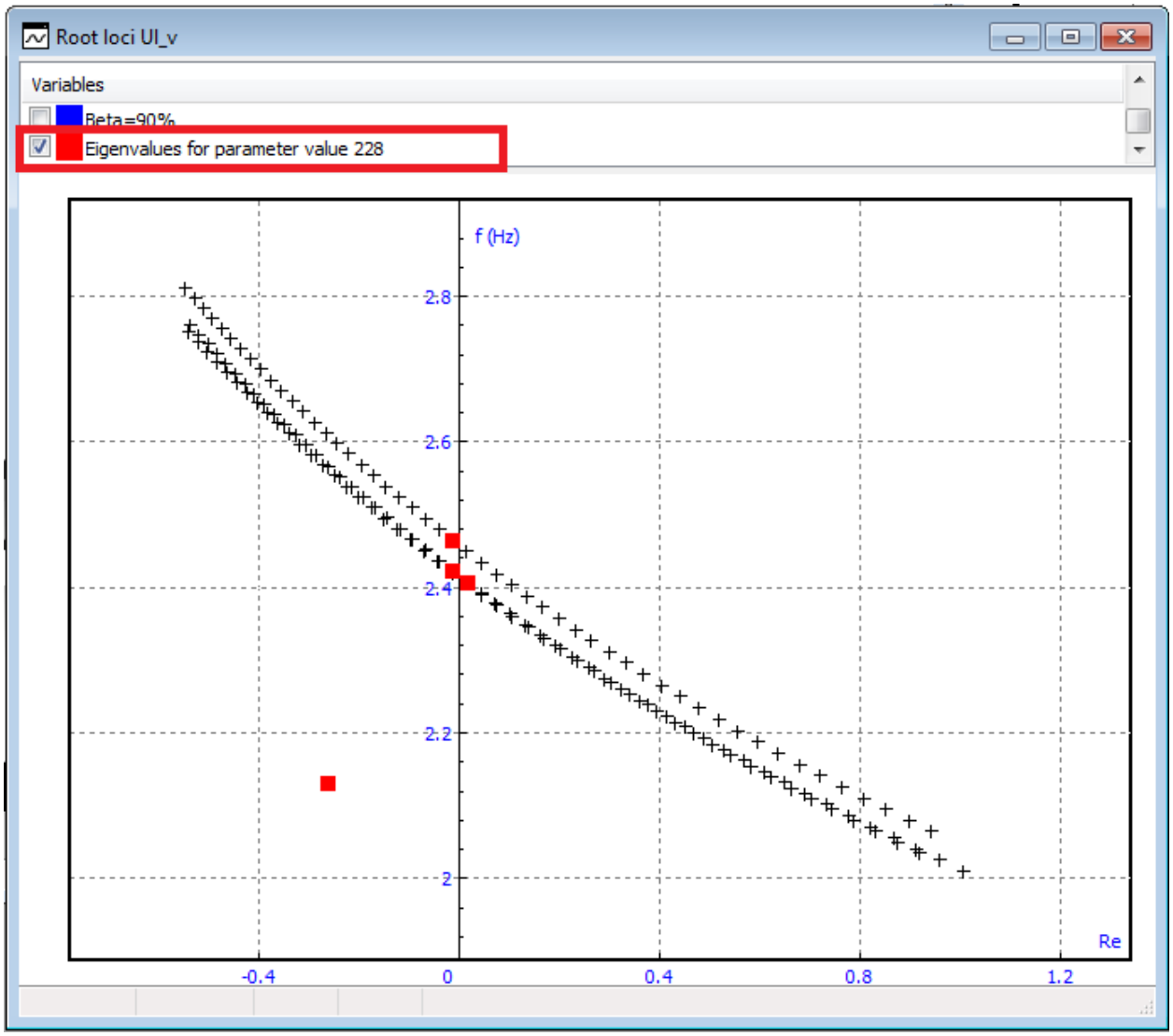

Figure 1.75. Stability bounds

Remark 1. In this test we have set moments of inertia of the frame, which give close values of eigenvalues or rotation about X and Y axis to the eigenvalue for the vertical degree of freedom. In this case the stability bounds for these degrees of freedom are almost the same. If you change the frame inertia parameters, stability results will differ from the theoretical one because the stability for rotational degrees of freedom will differ from the levitation.

Remark 2. Theoretical stability results in Section 1.6.5 can be applied with the model of bogie with rigid coupling of magnets with frame. The results cannot be directly valid for bogie models with a primary suspension, and numerical stability analysis with SLA tool is required.

1.10.4. Spring/damper magnet model as identifier control

Here we consider a simple model of levitation as an example of user's models of magnet force.

1. Load the model {UM Data}\Samples\MagLev\Bogie_6DOF.

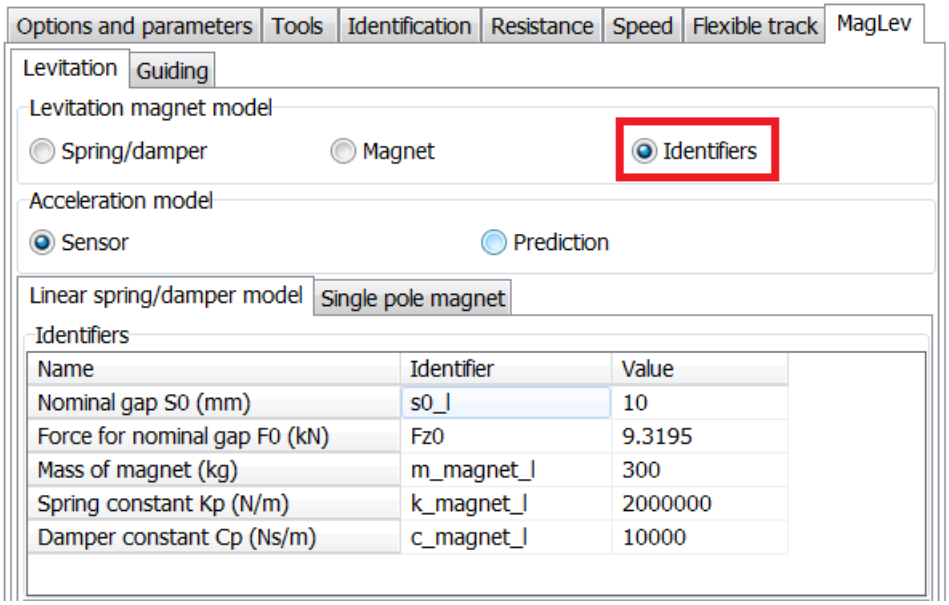

Figure 1.76. Levitation model by identifiers

2. Read the *Identifier control* configuration. The model is at v=0 speed mode.

The levitation magnet model is **Identifiers**, the guidance magnets are spring/damper. Levitation spring-damper forces are computed by variables created in the wizard of variables, Figure 1.77. The variables are assigned for the force identifiers with the Identifier control tool, Figure 1.78. Please note that the **Compute after kinematics** option is used in the identifier control.

3. Run simulation. Initial position of the frame is shifted slightly from the equilibrium position, so that a transient process can be seen in the plot. Change the levitation magnet model to the **Spring/Damper** one and compare simulation results, which must completely coincide.

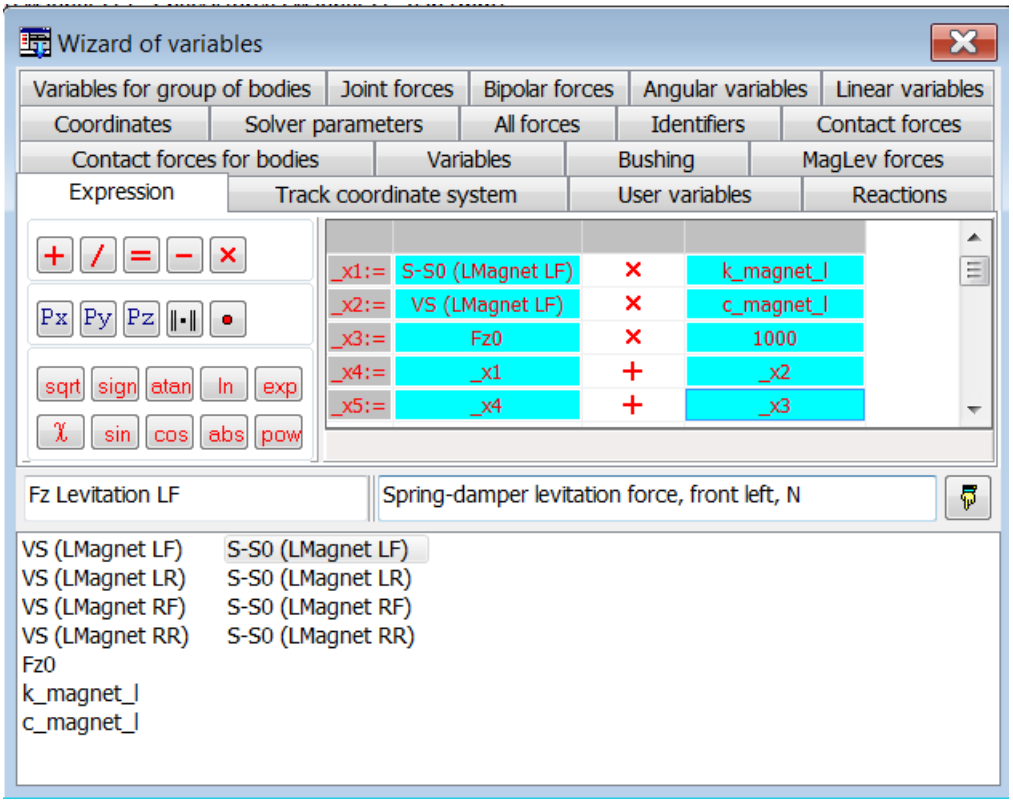

Figure 1.77. Variable for spring-damper magnet model

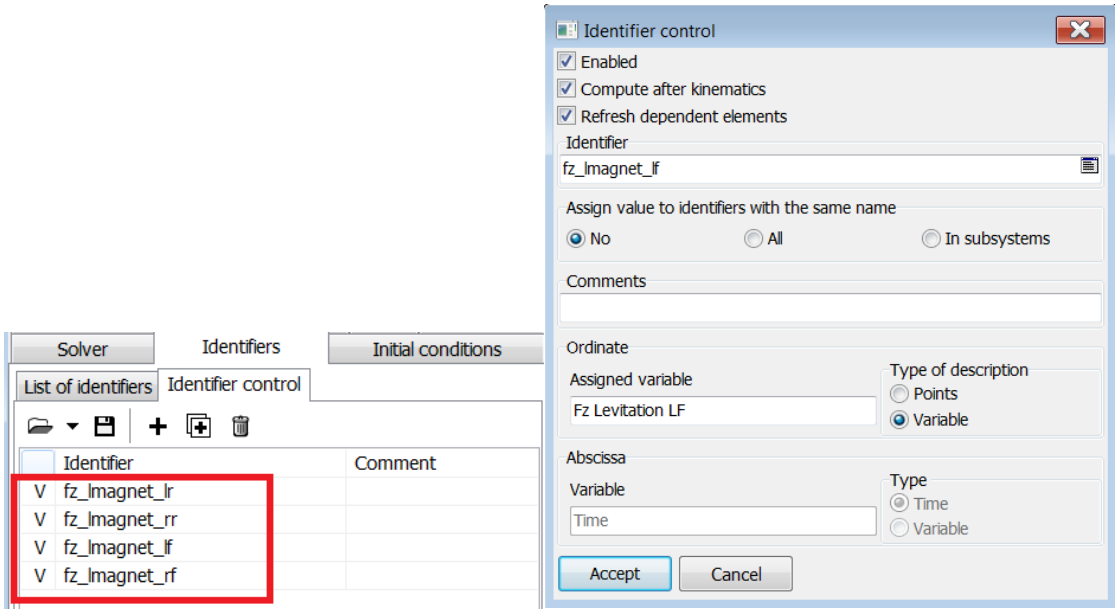

Figure 1.78. Identifier control for levitation force identifiers

1.11. References

[1] S.G. Meisenholder, and Wang, T.C., "Dynamic analysis of an electromagnetic suspension system for a suspended vehicle system," TRW Systems Group, Redondo Beach, Calif., 1972.

[2] M.L. Nagurka, and S.K. Wang, "A Superconducting Maglev Vehicle / Guideway System With Preview Control," *Journal of Dynamic Systems, Measurenent, and Control, ASME,* vol. 119, pp. 638-649, 1997.

[3] Y. Cai, and S. S. Chen, "A Review of Dynamic Characteristics of Magnetically Levitated Vehicle Systems," Energy Technology Division, Argonne National Laboratory, Argonne, Illinois, November 1995.

[4] Jin Shi, Wen-shan Fang, Ying-jie Wang, Yang Zhao, "Measurements and analysis of track irregularities on high speed maglev lines," *Journal of Zhejiang University-SCIENCE A,* vol. 15, no. 6, p. 385–394, 2014.

[5] S. Ren, A. Romeijn, and K. Klap, "Dynamic simulation of the maglev vehicle/guideway system," *Journal of Bridge Engineering,* vol. 15, p. 269–278, 2009.

[6] N. Hägele, and F. Dignath, "Vertical dynamics of the Maglev vehicle Transrapid," *Multibody Syst Dyn,* vol. 21, no. 3, p. 213–231, 2009.

[7] E. Gottzein, and B. Lange, "Magnetic suspension control systems for the MBB high speed train," *Automatica,* vol. 11, no. 3, pp. 271-284, 1973.

[8] R.Meisinger, Beiträge zur Regelung einer Magnetschwebebahn auf elastischem Fahrweg, Dr.-Ing Dissertation TU München, 1977.

[9] E. Gottzein, R. Meisinger, L. Miller, "Magnetic Wheel in the Suspension of High-Speed Ground Transportation," *IEEE Transactions on Vehicular Technology*, vol. VT. 29, no. 1, pp. 17-23, 1980.

[10] H. S. Han, "A study on the dynamic modeling of a magnetic levitation vehicle," *JSME International,* vol. 46, no. 4, pp. 1497-1501, 2003.

[11] G. Shen, R. Meisinger, and G. Shu, "Modelling of a high-speed Maglev train with vertical and lateral control," *Vehicle System Dynamics,* vol. 46, no. Supplement, p. 643–651, 2008.

[12] D. Pogorelov, "Zur Dynamik der Magnetschwebebahn. Institutsbericht IB-9," Institut B fuer Mechanik, Universitaet Stuttgart, Stuttgart, 1986.

[13] W. Brzezina and J. Langerholc, "Lift and Side Forces on Rectangular Pole Pieces in two Dimensions," *Journal of Applied Physics,* vol. 45, no. 4, pp. 1869-1872, 1974.

[14] W. Kortüm and P. Lugner, Systemdynamik und Regelung von Fahrzeugen, Berlin: Springer, 1994.

[15] C. F. Zhao, Zhai, W. M. and Wang, K. Y., "Dynamic responses of the low-speed Maglev vehicle on the curved guideway," *Veh. Syst. Dyn.*, vol. 38, no. 3, p. 185–210, 2002.

[16] H.-S. Han and D.-S. Kim, Magnetic levitation: maglev technology and applications. Springer Tracts on Transportation and Traffic, Dordrecht: Springer Science+Business Media, 2016.

[17] A. D'Arrigo and A. Rufer, "Design of an integrated electromagnetic levitation and guidance system for SwissMetro," in *EPE 99 - European Conference on Power Electronics and Applications*, Lausanne, Suisse, 1999.